
M.Sc. Thesis
Terrestrial Plant Fluorescence as seen
from Satellite Data

N. Khosravi

Referees:

Prof. Dr. John P. Burrows

PD Dr. Wolfgang von Hoyningen-Hühne

Institut für UmweltPhysik (IUP)

University of Bremen

Bremen, Germany

August 2012

I herewith declare that I did the written work on my own and only with the means as indicated.

Narges Khosravi

Acknowledgment

It would not have been possible to write this master thesis without the help and support of the kind people around me, to only some of whom it is possible to give particular mention here.

First and foremost, I wish to thank my parents, my sister and my cherished friends who stood by me as always and provided me with their unequivocal support and unconditional love which enabled me to be strong at the hardest of times. My mere expression of thanks to them does not suffice.

My deepest gratitude goes to my principal supervisor, Dr. Marco Vountas, without whose tremendous help, constant encouragement and lasting patience, this thesis would not have been possible. I wish to thank him for supporting me, believing in me and making me feel more like a colleague, a peer or a friend, rather than a pupil. I feel extremely lucky for having had the chance to work with him.

I wish to express my gratitude to my head supervisor prof. John P. Burrows for lighting the path through his prudent guidance and constructive suggestions. His wisdom and knowledge inspired and motivated me. I consider it an honor to be his student.

I would also like to thank my second supervisor, Dr. Wolfgang von Hoyningen-Hühne, who always supported me with his advice and did not hesitate to share his vast knowledge specially in aerosol retrieval and surface remote sensing.

I wish to thank Dr. Vladimir Rozanov, who is credited for developing the powerful radiative transfer model, SCIATRAN, employed in this research. He also kindly provided me with his unconditional support and shared his expertise in radiative transfer and remote sensing.

I also wish to thank DOAS group members, specifically Andreas Hilboll who shared an office with me, helped me in any possible way and remained my friend while I was working on the thesis.

I would like to thank all other people who contributed to my thesis including those whose works I have cited or provided me with technical assistance such as IT and aerosol groups at IUP.

Last but not least, I would like to acknowledge the academic and personal support of all my tutors and the staff of the University of Bremen and I wish to reminisce all IUP members and the PEP team for their friendly collaboration and encouragement, specially Dr. Annette Ladstätter-Weißenmayer, Anja Gatzka and Lars Jeschke for kindly and patiently supporting me from the beginning of the postgraduate program to the end.

*This dissertation is dedicated to the memory of Dr. Mohammad
Sepehr.*

Abstract

Among all the planets in the solar system, Earth has a different atmosphere with significantly less CO₂ and more O₂ and is the only *living planet*. Plants are known to be responsible for this special atmosphere. Their role in life, is not only limited to CO₂ absorption and O₂ emission. Plants also produce sugar as the first block of the food chain on Earth during the photosynthesis, save the soil from erosion, and regulate the temperature at the ground level.

Photosynthesis occurs by absorbing the sunlight and CO₂ from the environment, and releasing O₂ as a side product to produce food, i.e. sugar. Another side product of photosynthesis is the excess solar energy which is not used for photosynthesis. This energy can be re-emitted as fluorescence. Thus, when plants are experiencing any kind of stress which leads to less photosynthesis, the fluorescence emission increases. Therefore, fluorescence detection can help to identify changes in plant systems even before any visible symptom begins to appear (Joiner et al., 2011).

Terrestrial solar induced vegetation fluorescence has been detected for years in situ, airborne based and remotely from space-borne instruments. The advantage of space-borne fluorescence measurement is that it is fast and global. In this M.Sc. project a new fluorescence retrieval method, based on space-borne measurement is modeled and tested on real measured data by Scanning Imaging Absorption Spectrometer for Atmospheric CHartographY (SCIAMACHY) on Environmental Satellite (EnviSat). The radiative transfer model chosen for modeling the fluorescence as detected at Top Of Atmosphere (TOA) is SCIATRAN V3.1, including a fluorescence module both are developed by Rozanov (2011). The retrieval method is chosen to be Differential Optical Absorption Spectroscopy (DOAS) which is relatively simple and fast. It fits the best curve, by least square fitting, to the spectral features and proposes a fit factor for them. The created data by simulating the radiative transfer at TOA, as detected by SCIAMACHY which has a spectral resolution of $\sim 0.48 \text{ nm}$ for the wavelength of interest for fluorescence retrieval, was used for fluorescence retrieval at the first step. The fit factor was optimized by calibrating the method for variation of geophysical measurement terms. For the most adequate geophysical calibration the obtained fit factor is equal to 1.00 which means the fluorescence reference spectrum should not be scaled to fit the retrieved fluorescence.

Then the sensitivity of the fit is tested by varying all the known dominating factors and checking their influences on the retrieval outcome. As fluorescence adds an offset to the retrieval, the most important affecting terms are related to the measured brightness e.g. solar zenith angle and ground reflection. The reason is that the weight of an additive offset decreases by increasing the surface brightness. Respectively, a thorough error study is done to ensure the feasibility of the method in fluorescence retrieval. The model study is ended by testing the results on a short element of the spectral wavelength window, with a higher spectral resolution than SCIAMACHY (Kurucz et al., 1984).

The model study gave promising results. Thus, the method applied on the data measured by SCIAMACHY and the obtained fit factors were mapped and showed relatively reasonable values for fluorescence retrieval. The vegetated regions showed larger values than the sparsely vegetated regions. However, the results are still relative and are difficult to be interpreted quantitatively.

Contents

1	Introduction	1
1.1	Motivation	1
1.2	Fluorescence retrieval	2
1.3	The necessity and objectives of this study	3
1.4	The study pathway	4
1.5	Outline	4
2	Theoretical background	7
2.1	Photosynthesis and fluorescence	7
2.2	Radiative transfer	11
2.2.1	Light extinction term	12
2.2.2	Fluorescence emission	15
3	Methods and Data	19
3.1	SCIATRAN	19
3.2	DOAS	20
3.3	SCIAMACHY as the data source	23
4	Model study	27
4.1	Wide spectral window model study	27
4.1.1	Step 1: Finding the best fitting window	27
4.1.2	Step 2: Producing the fluorescence reference spectrum for DOAS	28
4.1.3	Step 3: The sensitivity study	28
4.1.4	Step 4: DOAS; feasibility study	30
4.1.5	Step 5: DOAS; calibration	30
4.1.6	Step 6: Sensitivity study considering RRS and the error study	32
4.1.7	Discriminating between vegetation fluorescence and other lu- minescence signals	34
4.2	Selected spectral window Model study	37
4.2.1	The effect of albedo	38
4.2.2	The effect of solar zenith angle	41

4.2.3	The effect of aerosols	41
4.2.4	Special case; simulation 1: Sahara	43
4.2.5	Special case; simulation 2: Polar regions	43
5	SCIAMACHY data study	47
6	Summary conclusion and outlook	51
A	Geophysical space-borne measurement geometrical properties	55
	Bibliography	61

Chapter 1

Introduction

1.1 Motivation

Earth is born approximately 4.54 billion years ago. Almost 3.80 billion years ago the first signs of life showed up as simple cells. Whereas, the land plants have appeared on earth only between 450 and 500 million years ago and it took almost 300 million years until mammals emerged. Nowadays our life on Earth is totally dependent on the unique environment which is built up by plants on the planet. They changed the Earth's atmosphere to a special atmosphere containing a large portion of oxygen. They are also the base of almost all the organic materials which we consume as food. Moreover, plants are affecting the daily weather and longterm climate, acting as a CO₂ absorber and temperature stabilizer, due to their growth/death rate and changing the ground reflectance. They play an important role in protecting Earth from global warming, or extreme cooling/warming on the daily basis. Therefore, to us as humankind, protecting the Earth's biosphere means protecting ourselves from extinction. In this hope, observing the vegetation behavior is a vital issue currently. Plant's responses to the environmental changes can also be a good indicator of regional anomalies. The main task done by plants is photosynthesis, in which carbon-dioxide and light are absorbed from the environment and oxygen is released. Therefore, photosynthesis has been an important focus of botanical studies. Studies show that all the sunlight absorbed by a plant's leaf cell, is not used for photosynthesis because of the energy mismatch. The excess energy is emitted to the space as fluorescence. Thus, the amount of emitted fluorescence is an indicator, showing how well the photosynthesis can be performed by the plant cell. This means while photosynthesis is going on, the emitted fluorescence can be used as a photosynthesis quality evaluator. This possibility makes the fluorescence emission very important in climate observations, because by measuring the fluorescence signals, some changes in plant systems can be identified even before any visible symptom begins to appear. For example, according to [Joiner](#)

et al. (2011) fluorescence observation is practically very important because it may provide vegetation stress sensation even before chlorophyll reductions take place. Several ways of vegetation fluorescence measurements have been proposed; in situ and remote measurements.

1.2 Fluorescence retrieval

For decades, the intensity of vegetation fluorescence radiation has been measured either from the ground, in laboratory, or from aircraft (see e.g., the review of Meroni et al. (2009), and the references therein). Thus, fluorescence retrieval has been done for a long time in situ or in a regional scale from air-borne instruments. Recently it has been proven that terrestrial vegetation fluorescence can also be measured from space by satellites. The importance of space-borne observation is that it has global coverage. Therefore it can lead to an evaluation of the global instantaneous vegetation carbon-related processes (Joiner et al., 2012).

Guanter et al. (2007) developed a new methodology of vegetation fluorescence estimation from space-borne and air-borne instruments. The method was applied on images acquired by Medium Resolution Imaging Spectrometer (MERIS) (European Space Agency, 2012b) on ENVIRONMENTAL SATellite (ENVISAT) (European Space Agency, 2012a) and launched by European Space Agency (ESA). The O₂-A absorption band was selected to be utilized for fluorescence retrieval. Their method was validated, being tested on images taken by a hyper-spectral airborne imager.

Later Guanter et al. (2010) measured the solar induced vegetation fluorescence at O₂-A and O₂-B absorption bands, using MERIS, to make it recognizable from reflected radiation.

As an outstanding in situ fluorescence measurement, Rascher et al. (2009) demonstrated a path to measure vegetation fluorescence directly. They also showed how this measurement can be used for a better estimation of leaf and ecosystem carbon fixation. They also provided a fluorescence spectra for velvet grass, bean, etc.

In 2010 solar induced vegetation fluorescence was retrieved with a high accuracy by MODTRAN5 beta which is a narrow band atmospheric radiative transfer model. Mazzoni et al. (2010) simulated canopy fluorescence by the model and fitted the fluorescence by cubic-spline fitting functions. So, they could retrieve the fluorescence without applying several initial constraints on the reflectance terms.

Frankenberg et al. (2011) have analyzed the effect of solar-induced chlorophyll fluorescence on space based high resolution spectra of reflected sunlight in the O₂-A absorption band. They showed that so far it is not possible to discriminate the effect of fluorescence on this spectral band from the impact of atmospheric scattering. So

neglecting fluorescence leads to unexpected substantial errors in the retrieved spectra. They also proposed an algorithm to decouple fluorescence from the scattering impact in the retrieval.

Joiner et al. (2011) and Frankenberg et al. (2011), measured the solar-induced vegetation fluorescence from Thermal and near-infrared Sensor for carbon Observation - Fourier Transform Spectrometer (TANSO-FTS) on the Greenhouse Gases Observing Satellite launched Feb. 2009 (GOSAT) measurements. They used filling in of a potassium solar Fraunhofer line near 770 nm for this purpose. They also made a global fluorescence map and its seasonal variation for the first time.

Again, Joiner et al. (2012) retrieved fluorescence from space using potentially lower-cost hyper-spectral instrumentation than GOSAT. They simulate the filling in of the calcium (Ca) II solar Fraunhofer line near 866 nm. They tested their results using the SCanning Imaging Absorption spectrometer for Atmospheric CHartographY (SCIAMACHY) space-borne instrument. They also compared variations of GOSAT and SCIAMACHY additive signals with the Enhanced Vegetation Index (EVI) from the MODerate-resolution Imaging Spectroradiometer (MODIS). It has been shown that the observed filling-in signal from SCIAMACHY is extremely weak at 866 nm, but there is a clear contribution between the spectral features and vegetation source.

1.3 The necessity and objectives of this study

This study is based on space-borne measurements at Top Of Atmosphere (TOA) that the terrestrial plant fluorescence can be measured by measuring its influence on the total spectral features (see section 2.2). SCIAMACHY launched on ENvironmental SATellite (ENVISAT) by European Space Agency (ESA) is chosen as the space-borne instrument for fluorescence retrieval in this study.

Terrestrial vegetation fluorescence, as can be seen in Fig. 1.1 is known as a broad-band spectral feature, applying an infilling-behaved light signature and an offset level to the retrieved light intensity at TOA.

Vountas (1999) and consecutive studies showed that it is possible to use a retrieving method for such an infilling of spectral features. Hence, the objectives of this study are:

- To develop a simple and fast retrieval method for fluorescence signal.
- To check how sensitive is the retrieval to geophysical and measurement parameters.
- To assess the method by applying it on real data measured by SCIAMACHY.

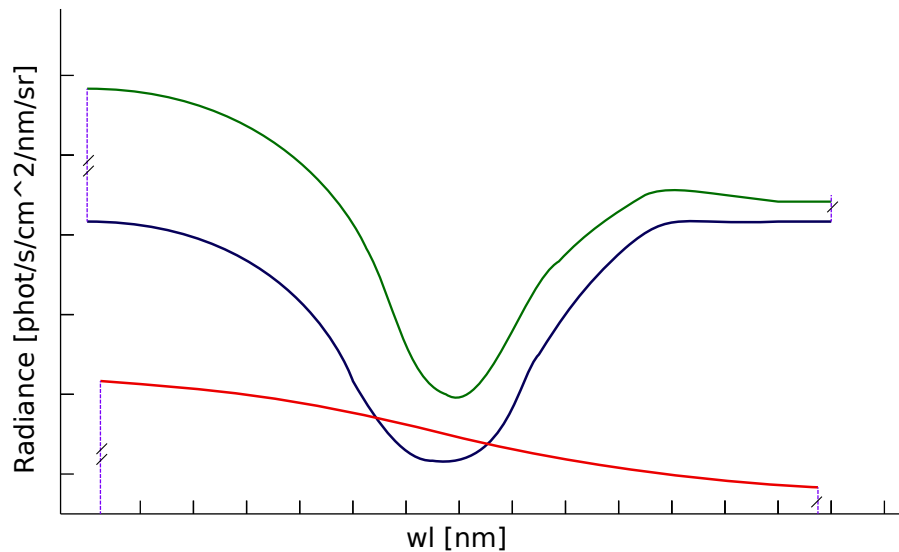


Figure 1.1: The vegetation fluorescence impact on the retrieved light at TOA. The *blue* curve represents a single spectral feature. Fluorescence radiance is shown in *red* and the *green* curve shows how the vegetation fluorescence adds a steep offset to it due to its slope.

1.4 The study pathway

According to Fig. 3.1 this study consists of two main parts:

- The model study:

A thorough model study has been done to find the best retrieving spectral wavelength windows, as deep absorption lines can dominate the fluorescence signal easily. The next objective of the model study was to find the most dominating environmental and geophysical factors on the retrieved fluorescence. For these purposes, a radiative transfer model, including a fluorescence module is required. The radiative transfer model, used in this study is SCIATRAN V3.1 provided by [RozaNov \(2011\)](#). The retrieving method has been chosen to be Differential Optical Absorption Spectroscopy (DOAS) which is simple and fast.

- The data (SCIAMACHY) study:

The data measured by SCIAMACHY instrument has been used in DOAS as well as the modeled spectral features.

1.5 Outline

This thesis contains 6 chapters, which are as follows:

- Chapter 1 is an introduction to the importance of the issue, a summary of the most important steps taken before, and a brief explanation about the necessity of this research. The objectives of the work are given afterwards.
- Knowing the importance of the issue and the historical background of vegetation fluorescence retrieval, chapter 2 consists of the background information which is necessary for this study. This chapter is divided into two main sections which are the physical and biological information about photosynthesis and its relation to the fluorescence emission, as the retrieval subject, and the radiative transfer section explaining the physics behind space-borne spectral measurements.
- After the scientific background, some basic information about the used method and the instrument as the source of data is given in chapter 3. This chapter consists of the radiative transfer model, utilized for simulating the satellite measurements, the method we have chosen to retrieve fluorescence with, and some information about the space-borne measurement instrument, as the source of data.
- Stepping into the first part of the study, chapter 4 is divided into two main sections. In the first section the main steps of the model study are explained. These steps are followed by some example model study results to illustrate the general ideas and concepts. The second section is a sequence of the first one, but is focused on a very small wavelength spectral interval.
- After retrieving the vegetation fluorescence successfully within the model study, finally in chapter 5, the developed method is applied on the real radiances, measured by SCIAMACHY in two different levels of complexity. Moreover, the obtained results are discussed and mapped.
- Chapter 6 is divided into a brief summary of the study, conclusion, consisting of the main outcomes, unknowns and the problems ahead, and an outlook part suggesting the necessary steps to be proceeded to solve the problems and validate the results. Indeed, some possible applications of the study are discussed in the final part.

Chapter 2

Theoretical background

2.1 Photosynthesis and fluorescence

The required knowledge necessary to develop *space-borne fluorescence retrieval*, is first, to understand the fluorescence emissions and how it contributes to photosynthesis, and second, to know the characteristics of the light, as it reaches to the TOA and received by the instrument.

Most of the visible solar light can reach the ground which is covered by natural surfaces. When a plant leaf cell receives a photon with a sufficient amount of energy for photosynthesis, it captures it as the main energy source for photosynthesis to produce oxygen and sugar as the main food block for all creatures. The emitted oxygen is taken by animals during the respiration as well as their released CO₂ is taken again into the (day-time) photosynthesis progress, forming the life cycle over the land.

Having a closer look to a plant leaf, as it can be seen from Fig. 2.1, most leaves consist of two epidermic layers and a Mesophyll layer in between, which holds chloroplast. Chloroplasts are the cells, filled with a liquid known as stroma, containing some pancake shaped objects called Thylakoid. Fluorescence emission due to photosynthesis occurs in the Thylakoid membrane which holds Chlorophyll-a and -b molecules (shortly Chl-a and Chl-b) knowing as photosynthetic pigments. From the quantum mechanics point of view, any molecule can absorb specific energy quantum with respect to its energy levels. Accordingly, Chlorophyll (Chl) pigments are able to absorb blue and red wavelength photons but not green light. Therefore, due to the back-reflecting of the photons, having green spectral wavelength, they appear to be green. The absorbed photon excites these molecules to higher energy levels. The Chl energy increases to the first singlet state absorbing red light and the second singlet state by blue light absorption. The high-energy second singlet state has a life-time of only 10^{-12} s and is too unstable to do any chemical work. Therefore, Chl usually loses the excess energy as heat by vibration-rotation and descends to the first singlet state.

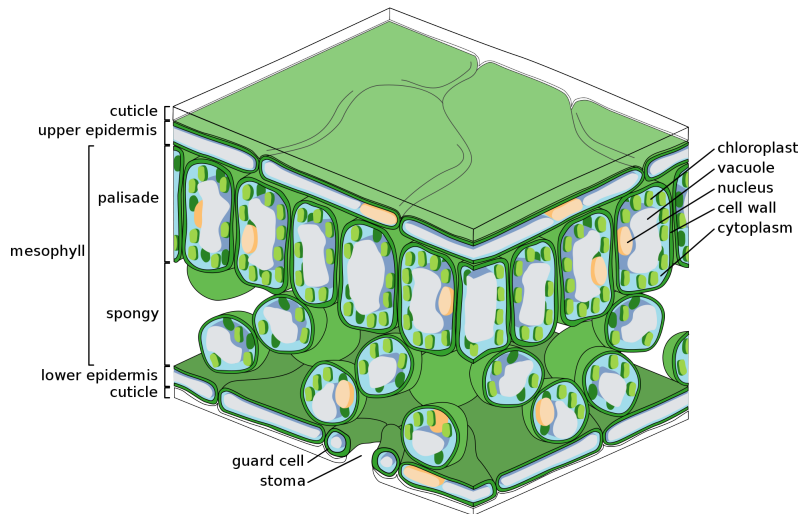


Figure 2.1: The leaf structure; epiderm, the Mesophyll and the chloroplasts are shown (Wheeler, 2010)

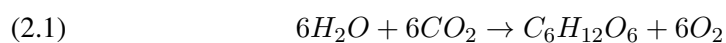
The first singlet state is much more stable than the second one having the life-time of 4×10^{-9} s (Heldt and Piechulla, 2010).

Having excited Chl molecules in first singlet state, the plant can do chemical work known as photosynthesis as the most important way of descending to the ground state. But there are some other ways to release the excess energy. As it can be seen from Fig. 2.2, releasing the excess excitation energy in the form of heat, the Chl molecule can reach an excited state of lower energy, called the first triplet state. The probability of reaching triplet state is low and therefore, the triplet state is relatively stable. Therefore, the molecule loses the rest of energy by emitting phosphorescence with the life-time of 10^{-4} to 10^{-2} s.

Fig. 2.2 also shows another possible way of excess energy release, known as fluorescence. Fluorescence is emitting the excitation energy back in the form of photons. As part of the excitation energy is usually lost beforehand as heat, by vibration and rotation, the fluorescence light has less energy, or longer wavelength, than the energy of the excitation light for attaining to the first singlet state.

From the total absorbed light, only 1-5% turns to fluorescence emission. The overall shape of vegetation fluorescence is illustrated in Fig. 2.3 and has two maxima around 680 and 740 nm (Bracher, 2012).

Photosynthesis is a chemical reaction as follows;



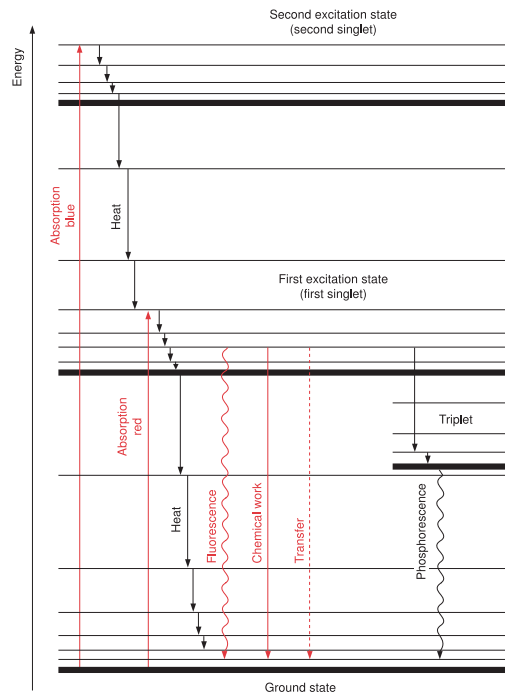


Figure 2.2: The energy levels of a Chl; First and second singlet states are shown which occur by absorbing red and blue light. Fluorescence, phosphorescence, and heat emission are also shown as the energy emission ways from the excited states to the lower energy states. (Heldt and Piechulla, 2010)

Standard spectrum of chlorophyll a in 90% acetone

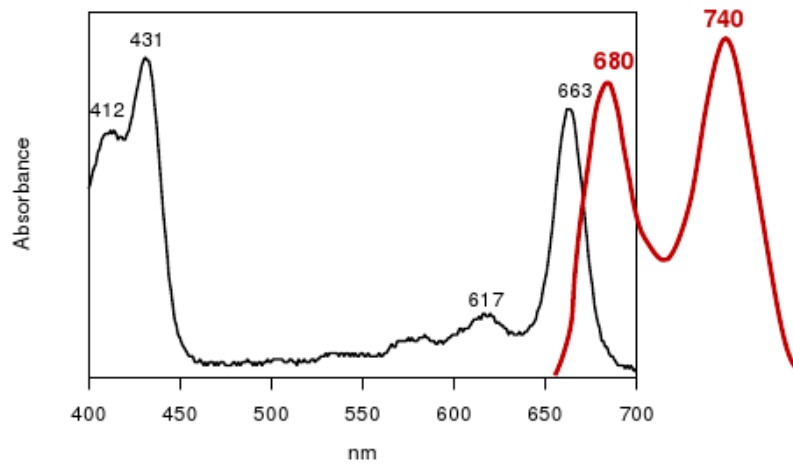


Figure 2.3: The fluorescence emitted from Chl-a has two emission peaks based on two main absorption peaks, having lower energy. (Bracher, 2012)

Interestingly, photosynthesis reaction has two main parts as well as the word *photosynthesis* itself consists of two main parts of *photo-* and *synthesis*; the light reaction (photo absorption and water depletion) and the dark reaction (synthesizing sugar):

- Light reaction:

According to Fig. 2.4 and Eq. 2.1, the light reaction, happening in the thylakoid membrane, is a part of photosynthesis in which, sunlight is absorbed and used for depleting the water molecules. The output of this part is oxygen emitted from the leaf epiderm. The products of this parts are Nicotinamid Adenin Dinukleotid PHosphat (NADPH) and Adenosine Triphosphate (ATP) molecules, being used as energy carriers.

- Dark reaction

Also known as Calvin cycle* or carbon-fixation reaction, is a part of photosynthesis in which NADPH and ATP molecules, being released into the stroma of the chloroplast, are used to produce sugar using the up-taken carbon dioxide. Light does not play a role in this step. Therefore, it's called dark reaction.

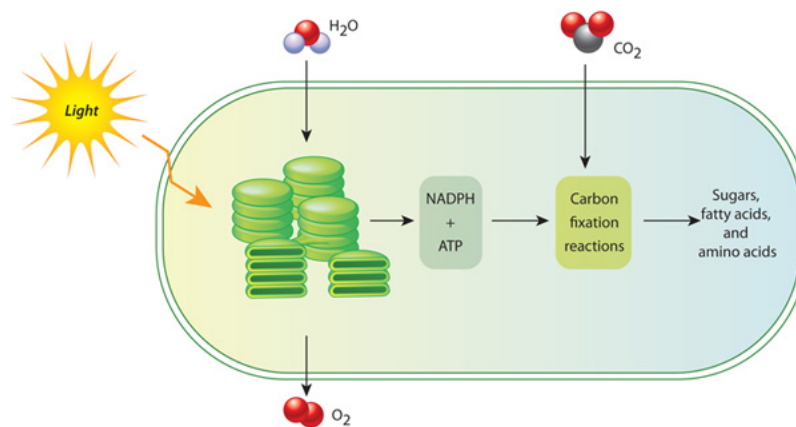


Figure 2.4: The light reaction and dark reaction; During the light reaction the sunlight is absorbed and fluorescence is emitted. The light reaction products e.i. ATP and NADPH are used as energy units in carbon fixation using CO₂ to produce sugar(NatureEducation webpage, 2010).

The light reaction is the part in which fluorescence emission happens. The Kelvin cycle is not directly related to fluorescence emission and can be ignored in this work.

*In the memory of v Melvin Calvin who is one of the scientists who discovered this cycle. His other colleagues were James Bassham, and Andrew Benson at the University of California, Berkeley Bassham and Calvin (1957).

As it has been mentioned above, the light reaction happens in the thylakoid membrane within the so-called photo-systems (PS). Photo-systems are made of a number of Chl molecules. Photo-system I (PSI) and photo-system II (PSII) are two different systems which can exist in a thylakoid membrane. Fig. 2.5 shows a schematic image of them. PSI can exist independently from PSII and contains much more Chl-a than Chl-b (in some cases no Chl-b at all). It is called PSI only because it is the PS which is discovered first but its main absorption peak is near 700 nm and is mainly responsible for the second peak of fluorescence emission double-peak curve on 740 nm as it can be seen from Fig. 2.3. In the other hand, PSII contains both Chl-a and Chl-b molecules (sometimes equally) and is mainly responsible for the first peak around 680 nm spectral wavelength (Bracher, 2012). In the following, vegetation fluorescence spectra, composed of both peaks, known as \mathcal{F} , is used in this study.

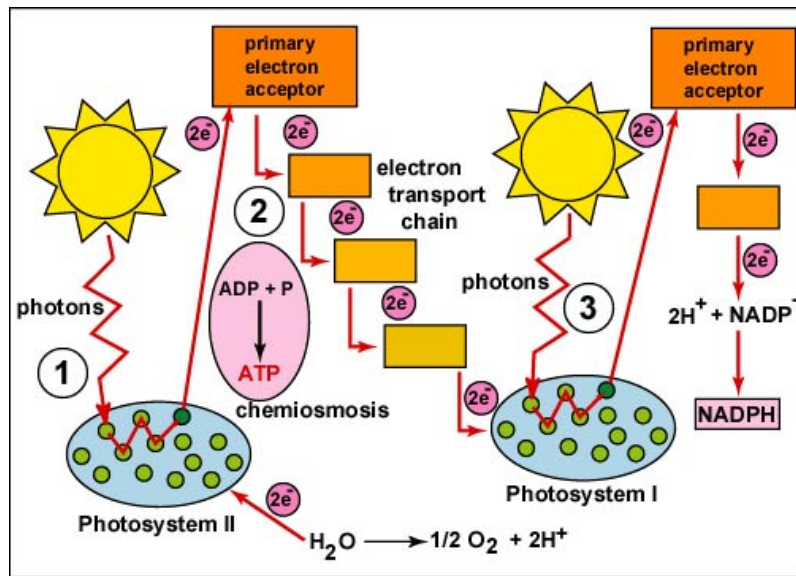


Figure 2.5: PSI and PSII; PSI can exist independently from PSII (Kaiser, 2001).

2.2 Radiative transfer

The emitted fluorescence from the plants travels through the atmosphere to reach the satellite detector and is influenced by some atmospheric properties. To analyze the fluorescence contribution to them, these atmospheric characteristics and their influences should be studied. There are also some radiative transfer concepts and general definitions which are necessary to be explained;

Radiance: *Radiance, I* , at a point in a light path is the radiant flux in a given direction per unit solid angle per unit area, perpendicular to the direction of the light propagation and measured in [$W m^{-2} nm^{-1} sr^{-1}$].

Irradiance: *Irradiance, E* , is defined as the radiant flux per unit area of the surface. Irradiance, called also *radiant flux density*, is measured in [$W m^{-2} nm^{-1}$].

Radiative Transfer Equation: *Radiative transfer equation*, is a statement of the conservation of energy, including all the energy losses and gains associated with a group of photons moving through the atmosphere along the light path to the instrument detector direction.

The incident radiation is influenced by two main opposite processes; loss by attenuation along the light path, and gain by scattering along the path from the light beams initially traveling in other directions. Therefore the received light at TOA is a combination of these gain/loss processes affected by a weak additive effect from vegetation fluorescence as well.

As it can be seen from Fig 2.6 eventually, the general radiative transfer equation should consist of the light extinction terms (absorption & scattering) and emission terms (fluorescence, etc.). scattering and reflection terms can be both towards and outwards the detector's position. The radiative transfer equation is proposed in Eq. 2.2:

$$(2.2) \quad \frac{dI(\lambda)}{ds} = -(Extinction\ terms)I(\lambda) + (terrestrial\ fluorescence\ term) \\ + (scattering\ and\ reflection\ terms\ into\ the\ detector\ direction)$$

2.2.1 Light extinction term

When a light beam passes through an environment, filled with gas molecules and/or aerosol particles, The light intensity at the end of the light path depends on the initial intensity of the light, $I_0(\lambda)$, the length of the light path through the absorber/scatterers (s), absorption/scattering ability of the gas molecules, so called extinction cross section, σ_{ext} , [$cm^2/particle$], which is divided into two main terms of absorption cross section, σ_{abs} , and scattering cross section, σ_{scatt} , and the total concentration of the absorber/scatterers along the path (N) [$particles/m^3$]. Therefore, according to the Beer-Lambert's law the general light extinction term is written as:

$$(2.3) \quad I(\lambda, s) = I_0(\lambda)exp(-\sigma_{ext}(\lambda).N.s)$$

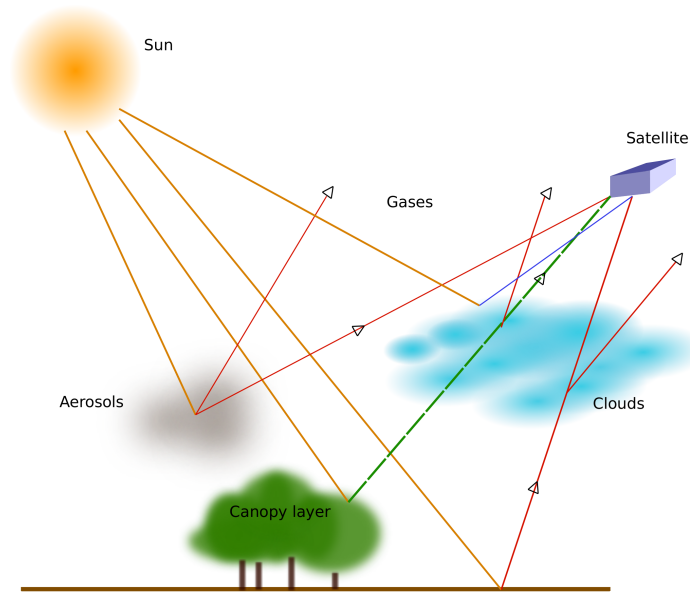


Figure 2.6: radiative transfer through the atmosphere. Extinction occurs by absorption and scattering which is shown in red. Fluorescence is colored green and the reflection from clouds can be seen in blue. Some scattering terms are into the satellite direction and some toward other directions.

The product of extinction cross-section and the length of the light path is also known as Optical Depth (OD).

The light absorption and scattering is defined as follows:

Absorption

Light absorption occurs when an incident photon collides with an atom/molecule is trapped and consumed to be converted into other forms of energy (Sadeghi, 2012). Absorption cross section, σ_{abs} , can be determined in the laboratory, so it is generally considered to be known at specific temperature and pressure.

In our case, the environment is Earth's atmosphere and the initial light intensity is the solar terrestrial radiation passing through the atmosphere. Earth's atmosphere is filled with Nitrogen (78.08%), Oxygen (20.95%) and some trace gases e.g., Argon, water vapor, ozone, methane, nitrous oxide, carbon dioxide. Each of these gases absorbs the light at some specific wavelengths due to their absorption cross section. Absorption is always paired with emission. Absorbing in a spectral wavelength leads to emission at a longer spectral wavelength with lower energy. Along the spectral interval of our interest (the land fluorescence emission interval 600-800 nm) the main absorbers are oxygen (O_2) and water vapor (H_2O).

Scattering

Beside absorption, another reason for light extinction is scattering. In general, the scattering process can be either *elastic* (preserving the incident energy) or *inelastic* (changing the incident energy) (Sadeghi, 2012). Elastic scattering is also divided into two main types of Rayleigh and Mie scattering with respect to the light and particles properties. Note that, scattering dominates the light received at TOA by both adding and subtracting photons to or from it.

Scattering features vary slowly, in contrast to rapid absorption fluctuations by wavelength variation. Light scattering occurs when a photon, during its interaction with a component of a medium, is scattered by the means of diverging from its original path.

Elastic scattering Elastic scattering is a scattering process in which the kinetic energy of an incident particle is conserved. This implies that the particle does not change the frequency of the light and only changes the traveling direction by changing the phase function. Note that, the scattering cross-section can vary with wavelength.

When a photon with a wavelength (λ) collides with a particle of a specific size, there are different scattering possibilities due to the particle size and wavelength: If the particle is much smaller than the wavelength of the photon, the scattering is divided evenly between the forward and backward direction with respect to the incoming photon direction. In this so-called *Rayleigh scattering* regime, the scattering cross-section, σ_{scatt} , is of the form:

$$(2.4) \quad \sigma_{Ray} = \sigma_{scatt}(\lambda) \sim \lambda^{-4}$$

Similarly, if the particle size is comparable with the wavelength, the scattering is strongly to the forward direction with respect to the incoming photon direction. In this so-called *Mie scattering* regime, the scattering cross-section, σ_{scatt} , is of the form:

$$(2.5) \quad \sigma_{Mie} = \sigma_{scatt}(\lambda) \sim \lambda^{-\kappa}, \kappa = 0..2$$

Inelastic scattering Elastic scattering plays an important role among the scattering types in the fluorescence retrieval. However, a non-negligible fraction of the scattered light is called *inelastic scattering*, which leads to redistribution of a small portion of photons over the wavelength. So it leads to some perturbation in spectral features by an energy shift of some photons to higher or lower frequencies. The released energy depends on the incident energy of the particle which is collided with the photon. To illustrate the level of complexity that such an event applies on our work, one can think of a photon with a specific wavelength colliding an atmospheric particle and shifting

to another spectral wavelength region due to its energy change. Inelastic scattering is known as Raman scattering.

In Raman scattering case a molecule is excited into a higher rotational or vibrational quantum state by an incident photon. The excited molecule then emits a photon of longer wavelength than the incident photon, with the energy difference being transferred by the molecule to the internal rotational or vibrational energy. If the molecule is already in an excited state, then it may emit a photon of slightly shorter wavelength than the incident photon and thereby return to its ground state and if not, the emitted photon has a longer wavelength. Depending on the way of energy loss, Rotational Raman Scattering (RRS) and Vibrational Raman Scattering (VRS) are two main types of Raman scattering.

Raman scattering is more important working on shorter spectral regions such as UV and does not play a significant role in longer wavelength intervals e.g. IR (Infra Red). In practice, however, as the atmospheric contribution of VRS compared to RRS in the UV-visible spectral ranges is very low, for the usual scientific purposes, the atmospheric VRS is often neglected (Joiner et al., 2012).

Rotational Raman scattering in the air is often referred to as the *Ring effect*, causing *filling-in* of Fraunhofer lines[†] in a daytime spectrum. The Ring effect, is responsible for approximately 4% of all scattering events occurring by the air molecules (Vountas, 1999).

Based on the explanation above, in this study, in setting up the atmospheric optical components of the retrieval process, only rotational Raman scattering has been taken into account, although its impact on the retrieved radiance is not significant, it correlates to the fluorescence retrieval, and should be tested through the retrieving method carefully.

2.2.2 Fluorescence emission

The main objective of this study is to retrieve plant fluorescence among all of the described spectral features. So the contribution of fluorescence to the total radiance is the key to retrieve fluorescence among other spectral features.

At the first glance it seems that there is no way to distinguish between such small fluorescence radiance and reflected/scattered light, as they are significantly stronger than fluorescence. However, the Fraunhofer lines can make it possible to separate fluorescence additive intensity and reflected/scattered light. From the fluorescence

[†]Fraunhofer lines are some narrow absorption lines in the sun irradiance spectra due to the absorption in the solar atmosphere. They are called Fraunhofer lines in the memory of the German physicist Joseph von Fraunhofer (1787–1826) who observed them for the first time. The intensity of some of them is less than 10% of the surrounding continuum (Elachi and van Zyl, 2010)

definition, light is absorbed at short wavelengths and re-emitted at longer wavelengths. Therefore, in principle, by comparing the depth of a Fraunhofer line relative to the continuum in the retrieved light and incident light the additive fluorescence radiation can be detected and measured as it is shown in Fig. 2.7.

According to Fig. 2.3 the terrestrial plant fluorescence is a double peak spectral feature, varying slowly in contrast to absorption features. Knowing the general behavior of the light traveling through the atmosphere, the fluorescence net effect on the received light at TOA is an additive offset as shown in Fig. 2.7. Therefore, due to its own structure, it changes the shape of Fraunhofer lines by adding an asymmetric offset to them due to its slope.

Thus, the net effect of fluorescence on the light intensity measured at TOA, so-called the relative fluorescence contribution to the light radiance is defined as the fluorescence reference spectrum, F :

$$(2.6) \quad F = \ln \frac{I^+}{I^-}$$

with I^+ and I^- are the total radiance detected by the instrument at TOA including and excluding fluorescence respectively. F is also defined as the fluorescence reference spectrum.

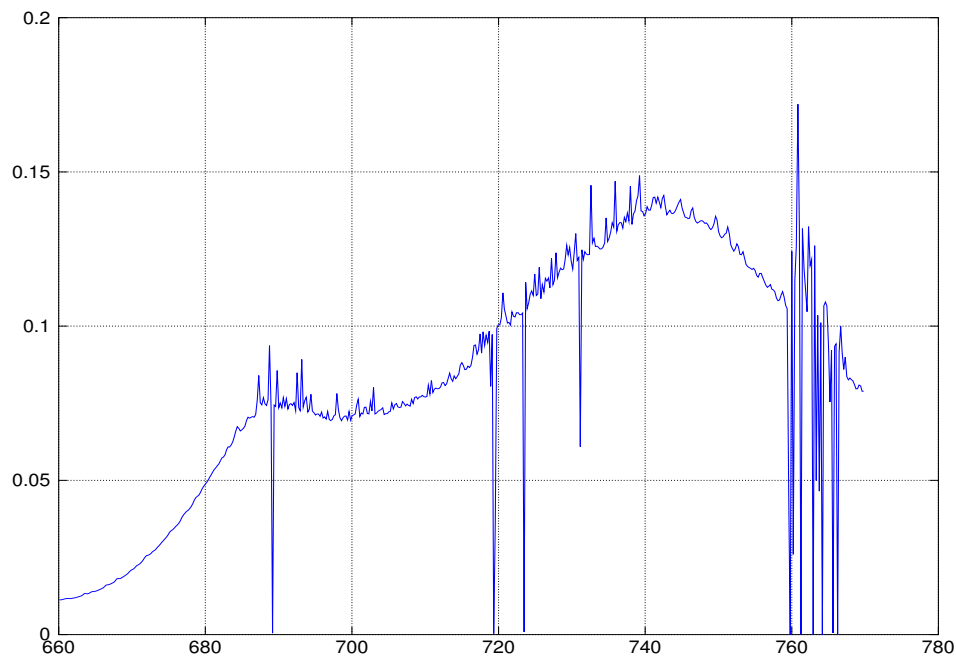


Figure 2.7: The fluorescence reference spectrum, F , is a unit-less quantity, showing how the fluorescence emission contributes to the radiance received at TOA. In other words, F defines the net effect of the additive fluorescence with respect to its shape. The center of the Fraunhofer lines are filled by fluorescence. Therefore, they are showing small peaks. Wherever there is a strong gas absorption within this wavelength window, the effect of fluorescence is difficult to be seen and $\frac{I^+}{I^-}$ is approximately one. So, the F value fluctuates strongly and goes to zero.

Chapter 3

Methods and Data

Knowing the major atmospheric properties, dominating the fluorescence retrieval at TOA, e.g. absorption and different kinds of reflection and scattering, a radiative transfer model can help to simulate the radiance received by the satellite instrument at TOA. According to Fig. 3.1 both radiances including and excluding fluorescence emission (I^+ and I^- respectively) are modeled using SCIATRAN, the selected radiative transfer model. This modeled radiances can be used in the retrieving method, DOAS in this case, as well as the real intensity coming from measurement at TOA. Looking at Fig. 3.1 the ratio of radiances in presence and absence of fluorescence is used to calculate fluorescence reference spectrum, F . In the model study part, F is coupled with I^+ , both created by the radiative transfer model to simulate fluorescence retrieval. However, applying the results on the real data, the radiance, I^+ , is measured by SCIAMACHY but utilized with F values created by the model.

3.1 SCIATRAN

SCIATRAN 3.1 is a powerful radiative transfer model designed as a software package, developed in FORTRAN95 by [Rozanov \(2011\)](#).

It is a software package which can be adapted to solve a wide range of scientific tasks. The program has been developed at the Institute of Environmental Physics (*IUP*), University of Bremen, Germany.

In general, SCIATRAN can model the radiative transfer from 175.44 nm to 40 micrometers. It also can model radiative transfer for any observation geometry as well as any location of the instrument (in the space, on the ground, within the atmosphere or under a water surface). Trace gases (O_3 , NO_2 , ClO, OCIO, BrO, HCHO, SO_2 , NO_3 , O_4 , O_2 , H_2O , CO_2 , CO, CH_4 , N_2O , NO, NH_3 , HNO_3 , OH, HF, HCL, HBR, and HI), Rayleigh scattering, aerosols and cloudiness can be chosen manually in SCIATRAN, and Lambertian reflection with wavelength dependence or constant



Figure 3.1: A schematic structure of the study pathway

ground reflection as well. Bidirectional Reflectance Distribution Function (BRDF) is available but an isotropic albedo is chosen in this study.

This version of SCIATRAN includes a fluorescence module, which allowed us to calculate radiative transfer of the vegetation fluorescence in the form of known spectra. This spectra will be considered by the program as an emission source located at the canopy layer. Currently, the used vegetation fluorescence spectrum is an emission spectrum of velvet grass at canopy level (Rascher et al., 2009). The spectrum, \mathcal{F} , has been scaled to a maximum value of $3.0 \text{ mW m}^{-2} \text{ sr}^{-1} \text{ nm}^{-1}$ (Rozanov, 2011) and can be seen from Fig. 3.2.

3.2 DOAS

So far, the radiative transfer model used for simulating the received radiance at TOA is introduced. The current question is how to retrieve vegetation fluorescence in the next step;

Differential Optical Absorption Spectroscopy (DOAS) (Platt and Stutz, 2007) is a fitting retrieval method originally, to determine the concentration of trace gases in the atmosphere, from remote sensing measurements of light in any selected windows in the UV, visible, and NIR spectral range. DOAS is based on Beer-Lambert's law of light extinction.

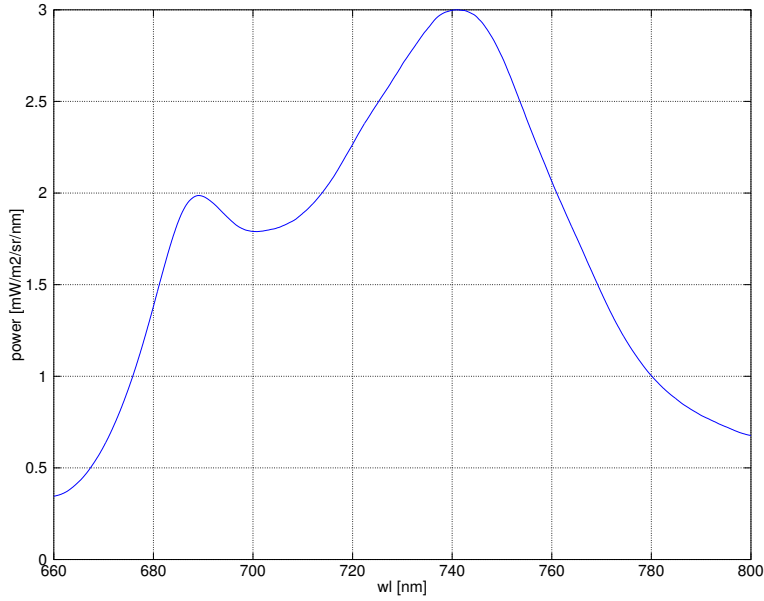


Figure 3.2: The fluorescence emission power from velvet grass at canopy level (Rascher et al., 2009).

DOAS discriminates between different absorbers based on their rate of variation with respect to the spectral wavelength. Gradual variations by wavelength, e.g. scattering, are fitted separately from fast variations such as absorption.

Knowing the absorption cross-section of different absorbers, DOAS separates the main absorbers by finding the best curve fitted to the retrieved spectral features. Scattering features should be taken out by fitting a polynomial to them. The main scattering terms are due to Mie and Rayleigh scattering which are discussed before. Thus, the Beer-Lambert's law for a general case is:

$$(3.1) \quad I(\lambda, \theta) = I_0(\lambda) \exp \left(- \int \sum_{j=1}^J \sigma_j(\lambda) N_j(s) + \sigma_{Ray}(\lambda) N(s) + \sigma_{Mie}(\lambda) N(s) ds \right)$$

where $I(\lambda)$ and $I_0(\lambda)$ are the measured radiances of the incident and the transmitted radiations, $N(s)$ is the number density of either molecules or aerosol particles and ds is the light-path differential element.

In the Eq. 3.1, the summation is over all the absorbers, depending on the type of gases which have absorption within the selected wavelength interval. Knowing the

$\sigma_{Ray}(\lambda)$ and $\sigma_{Mie}(\lambda)$, the scattering terms are turned to be polynomials with respect to the λ . Besides, the concentration of different species is not constant along the light path. If the absorption cross-sections are assumed not to vary along the light-path, the integration of N_j along the light-path can be defined as a new variable the *slant column density*, SC_j , which has the unit of [*molecules cm⁻²*]. summation on j is to consider each type of absorber particles.

$$(3.2) \quad SC_j = \int N_j(s) ds$$

Thus, Eq. 2.3 can be written as:

$$(3.3) \quad \ln \frac{I(\lambda, \theta)}{I_0(\lambda)} = - \sum \sigma'_j(\lambda) SC_j - \sum b_p^* \lambda^p$$

Each trace gas in Eq. 3.3 has an absorption cross-section of $\sigma'_j(\lambda)$ and a slant column of $SC_j(s)$.

Having the Eq. 3.3, known as general DOAS equation, some adjustments are required for being used in fluorescence retrieving:

$$(3.4) \quad - \ln \frac{I(\lambda, \theta)}{I_0(\lambda)} = \sum \sigma'_j(\lambda) SC_j + \underbrace{\sum b_p^* \lambda^p}_{\text{Raman scattering OD}} + \underbrace{\mathbf{f}F}_{\text{fluorescence OD}}$$

The fluorescence OD (Optical depth) term consists of

- "F" which is defined in Eq. 2.6 as fluorescence reference spectrum and acts as an pseudo emission cross section for DOAS method and
- "f" which is a DOAS fluorescence fit factor, and reacts like a fluorescence *column* showing how much the *pseudo emission cross section*, prepared by the radiative transfer model, should be scaled to represent the fluorescence OD on that certain ground pixel. The used reference spectrum is F as defined in Eq. 2.6.

The Raman scattering OD, which is known as RRS OD, is also consists of a Raman reference spectrum, R , and a Raman fit factor, r .

DOAS solves the equation above by fitting the best curve to each term, using the *least square fit*, which means the difference between the real points and the related fitted curve points should be minimized.

Note that, the emitted fluorescence experiences extinction by means of absorption as well as other light radiances. So the fluorescence radiance at TOA is not exactly

the same as the fluorescence radiance at the canopy layer, though the difference is not significant. Therefore, the fluorescence reference spectrum, F , was created based on the radiances modeled at TOA. So, the fluorescence extinction due to the absorption and scattering is also taken into account in F creation.

Therefore, the final DOAS retrieval method can be written as:

$$(3.5) \quad \left\| \tau(\lambda) - \sum_{j=1}^J \sigma'_j(\lambda) SC_j - r R - f F - \sum_{p=0}^M b_p \lambda^p \right\|^2 \rightarrow \min$$

$$\text{while } \tau(\lambda) = -\ln \frac{I(\lambda, \theta)}{I_0(\lambda)} = \ln \frac{I_0(\lambda)}{I(\lambda, \theta)}.$$

Finding "f" is the main objective of DOAS application, as it scales the retrieved fluorescence with respect to the modeled fluorescence emission cross section (fluorescence reference spectrum, F).

3.3 SCIAMACHY as the data source

The chosen instrument for this study is Scanning Imaging Absorption Spectrometer for Atmospheric CHartographY (SCIAMACHY) launched on the ENVironmental SATellite (ENVISAT), by European Space Agency, (ESA) from Kourou, French Guiana, in March 2002 and is out of order since April 2012. SCIAMACHY covered a wide wavelength range (from 240 nm to 2380 nm in eight channels), which makes it an ideal sensor for the detection of aerosols and clouds, as well as being suitable for several retrieval methods of trace gases. Besides it can observe an air volume from three different viewing angles (nadir, limb and sun/moon occultation), leading to precise atmospheric data. Furthermore, SCIAMACHY benefits from a relatively high spectral resolution, ranging from about 0.2 nm to 1.5 nm for its scanning channels over the range of 240 to 1700 nm, and also selected regions between 2000 nm and 2400 nm (Bovensmann et al., 1999)

ENVISAT is a polar, sun-synchronous satellite, flying at the mean altitude of 779.8 km with orbital period of 100.6 minutes and a repeat cycle of 35 days (501 orbits). The main objective of the SCIAMACHY instrument is the quantitative determination of the atmospheric constituents (trace gases) on a global scale with improved temporal and spatial coverages (Bovensmann et al., 1999).

A complete list of all channels and their proper spectral resolutions can be found in table 3.1. Among these channels, the fluorescence emission spectral interval is covered by channel four, cluster 26, so the spectral resolution is relatively high (~ 0.48 nm) and its spatial resolution in the selected channel (4) and cluster (26) is 30×240 km².

Table 3.1: An overview of the spectral channels of SCIAMACHY including the respective clusters and spectral resolution for each channel.

Channel Nr.	WL range (nm)	Cluster index	Spectral Res. (nm)
1 (UV)	214 - 334	1 - 6	0.24
2 (UV)	300 - 412	7 - 11	0.26
3 (VIS)	383 - 628	12 - 20	0.44
4 (VIS)	595 - 812	21 - 28	0.48
5 (NIR)	773 - 1063	29 - 35	0.54
6 (SWIR)	971 - 1773	36 - 47	1.48
7 (SWIR)	1934 - 2044	48 - 53	0.22
8 (SWIR)	2259 - 2386	54 - 56	0.26

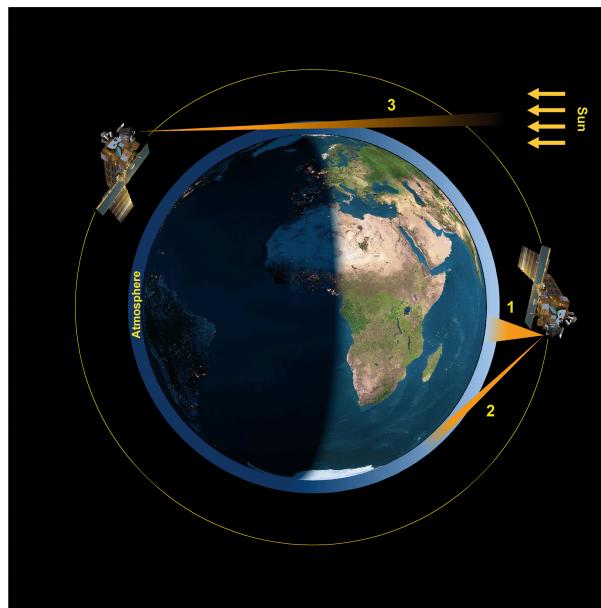


Figure 3.3: Scientific observation modes of SCIAMACHY: 1 = nadir (used for this study), 2 = limb, 3 = occultation. The picture was adapted from the recent SCIAMACHY book, by [Gottwald and Bovensmann \(2011\)](#).

Space-borne fluorescence retrieval can be utilized for a vast area of research and industry. From agricultural purposes to the observation of global vegetation cover. Any variation in global vegetation coverage can be important with respect to the global carbon cycle and climate models. Plants affect the Earth's climate by regulation the ground reflection and humidity. Therefore, their variation can be considered in the climate models. Specially, the outstanding property of fluorescence detection which enable us to predict the changes is particularly important in climate sciences and Earth observations.

Chapter 4

Model study

4.1 Wide spectral window model study

The general purpose of the model study before the SCIAMACHY data study was to find the best fitting windows, testing the sensitivity of the produced fluorescence reference spectrum, F , with respect to the main environmental and geophysical dominating factors, and to check for the capability of DOAS to retrieve terrestrial vegetation fluorescence. These have been done by taking the following steps:

4.1.1 Step 1: Finding the best fitting window

As fluorescence is a relatively weak offset over the total received radiance, deep absorption lines interfere with the fluorescence retrieval. Therefore, finding the suitable spectral windows within the fluorescence emission wavelength interval means finding a wavelength window containing the least atmospheric absorption lines. In order to find such a window SCIATRAN is used, including the solar irradiance, measured by SCIAMACHY and having the SCIAMACHY spectral resolution, all the main atmospheric absorbers and constant surface reflectance. The most dominating absorbers in the atmosphere within the fluorescence double peak wavelength interval are oxygen and water vapor. As it can be seen from Fig. 4.1 there are two main spectral windows which seem to be affected only by Fraunhofer lines but no deep absorption feature from oxygen and water vapor.

According to the Fig. 4.1 the main absorption-free windows are 660–683 nm and 745–758 nm . The second wavelength window, has been chosen for this study. From Fig. 4.1 it can be seen that the fluorescence spectral features are stronger in the second window, because of the relatively larger fluorescence values. Although, it is helpful to repeat the study for the first wavelength window as well, it has been not done in this study because of lack of time.

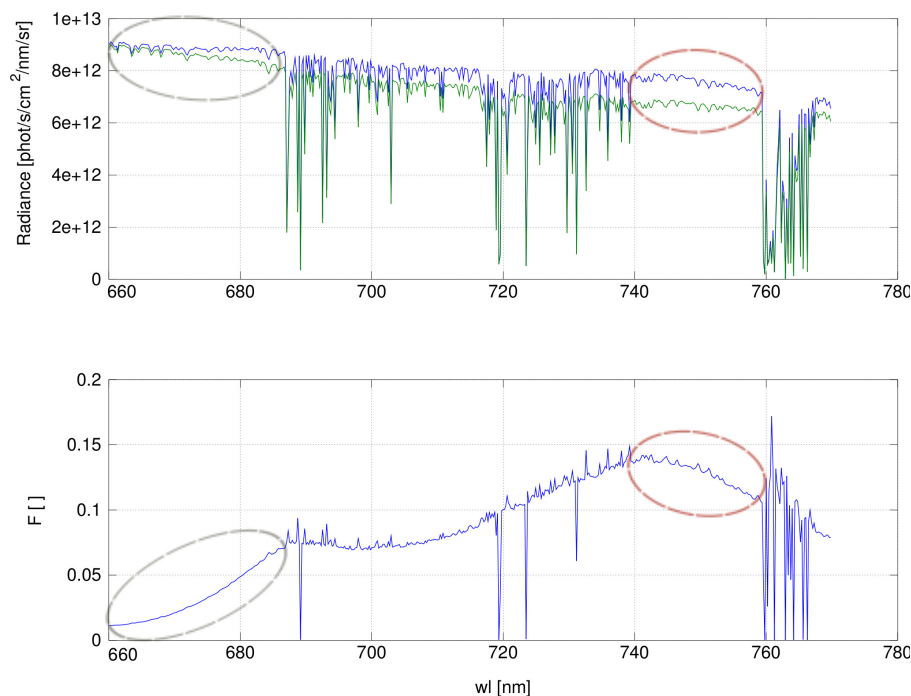


Figure 4.1: The spectral windows which are free of absorption are specified by ovals. The best fitting windows is shown a red oval for the radiance plot (upper) and fluorescence reference spectrum plot (lower). From F , one can realize that the spectral features are weak in the first window due to the small fluorescence radiance (upper).

4.1.2 Step 2: Producing the fluorescence reference spectrum for DOAS

After selecting a window with the minimum gas absorption lines, the next step is to produce fluorescence reference spectra. For this purpose, the ratio of I^+ to I^- , both produced by SCIATRAN, was calculated. Other geophysical properties for the creation of I^+ and I^- are always equal. This reference spectrum can be produced for different geophysical conditions e.g. high ground reflectance or different relative azimuth angles to analyze their effect on F .

As it can be seen from Fig. 4.2 the produced fluorescence reference spectrum shows the infilling-behavior and the steep offset level added by fluorescence on the simulated retrieved light intensity at TOA.

4.1.3 Step 3: The sensitivity study

The sensitivity study is to show how sensitive the fluorescence reference spectrum modeling is to the geophysical and environmental factors such as solar zenith angle or aerosol optical depth for any selected ground pixel in the real study. Therefore, in the model study we simulated the real condition by varying geometrical measurement

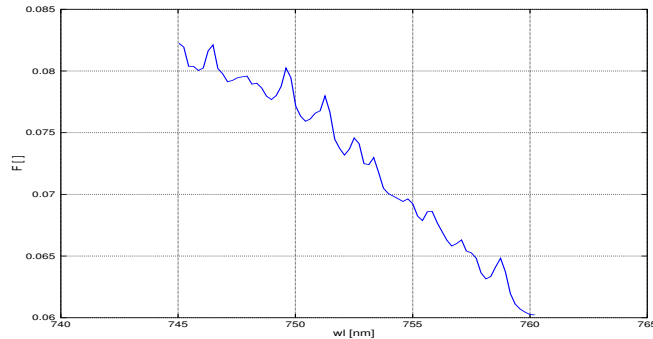


Figure 4.2: The infilling-behavior and the added steep offset the Fraunhofer lines can be seen on fluorescence reference spectrum within the selected wavelength window. The spectral window is about 2 nm extended in this plot from the original selected window ($745 - 758 \text{ nm}$) only because of technical reasons.

factors (see appendix A). The sensitivity study is to ensure all the dominating geophysical parameters on the fluorescence reference spectrum retrieval are considered. It also shows how important are the following factors respectively:

The ground reflection and solar zenith angle

increased ground reflection or small solar zenith angles are both increasing the brightness. As it can be seen from the fluorescence reference spectrum in Eq. 2.6 and 4.1, the higher background intensity I^- , the ratio of I^+ over I^- is closer to one, and the its logarithm is closer to zero. Thus, the fluorescence reference spectrum is more difficult to retrieve. This should be tested on the model. \mathcal{F} represents the fluorescence emission radiance, directly converted from fluorescence power shown in Fig. 3.2.

The effect of ground spectral reflectance on the fluorescence reference spectrum can be modeled by simulating the light intensity received by the satellite at TOA, in several different ground reflection percentages and a number of solar zenith angles, while other geophysical conditions are kept constant.

As can be seen from Fig. 4.3 the model results follows our expectation and fluorescence reference spectrum is turned out to be smaller when the surface reflection is stronger. According to the Fig. 4.3 the model results show stronger offset when the solar zenith angle is large and/or ground reflection, albedo, is not so strong.

The slope of fluorescence reference spectrum can be seen along the wavelength axis. The weakening of F is also shown with respect to the albedo variation. For high albedo values, F has significantly weaker features. In other words, more ground

reflection leads to smaller fluorescence reference spectrum.

$$(4.1) \quad \lim_{I^- \rightarrow \infty} \frac{I^+}{I^-} \sim \lim_{I^- \rightarrow \infty} \frac{I^- + \mathcal{F}}{I^-} = 1 + \lim_{I^- \rightarrow \infty} \frac{\mathcal{F}}{I^-} \rightarrow 1$$

The relative azimuth and viewing angles

As it has been mentioned before, SCIAMACHY's viewing angle varies between 0 and 30 degrees. According to the model study, the relative azimuth variation between 0 – 180 degrees within this small viewing angle interval does not apply any significant difference in fluorescence reference spectrum.

Fig. 4.4 shows that for the small viewing angle of 30.0 degrees, which is the largest viewing angle possible is nadir mode of SCIAMACHY, the relative azimuth angle variation has no significant effect on the modeled fluorescence reference spectrum retrieval. There is no significant color change along the azimuth angle axis which means for each wavelength, F remains unchanged with respect to the azimuth angle variation.

4.1.4 Step 4: DOAS; feasibility study

So far the model study was focused on the sensitivity of the fluorescence reference spectrum to different parameters. This step is to test the feasibility of DOAS to retrieve fluorescence. Thus, the fluorescence reference spectrum and the I^+ produced by SCIATRAN, as a replacement for a real radiance received by the satellite, were inserted into DOAS to retrieve f as the fluorescence fit factor. The output fulfilled the expectation that DOAS should be feasible for fluorescence retrieval as well as RRS retrieving showed by Vountas (1999).

The fitted fluorescence OD, produced by DOAS, is shown in Fig. 4.5. It can be seen that the fitted fluorescence OD and the product of fF are matching well for the model.

4.1.5 Step 5: DOAS; calibration

DOAS is prospected to retrieve fluorescence after the feasibility test. So far, it was important to ensure that all the important dominating environmental and measurement geometrical parameters are taken into account.

The main question for interpreting f is, what does the fit factor, f , tell about fluorescence retrieval? When fF exactly represents the fluorescence OD and no scaling is required, f , as the scaling factor is supposed to be one. Thus, when f is equal to

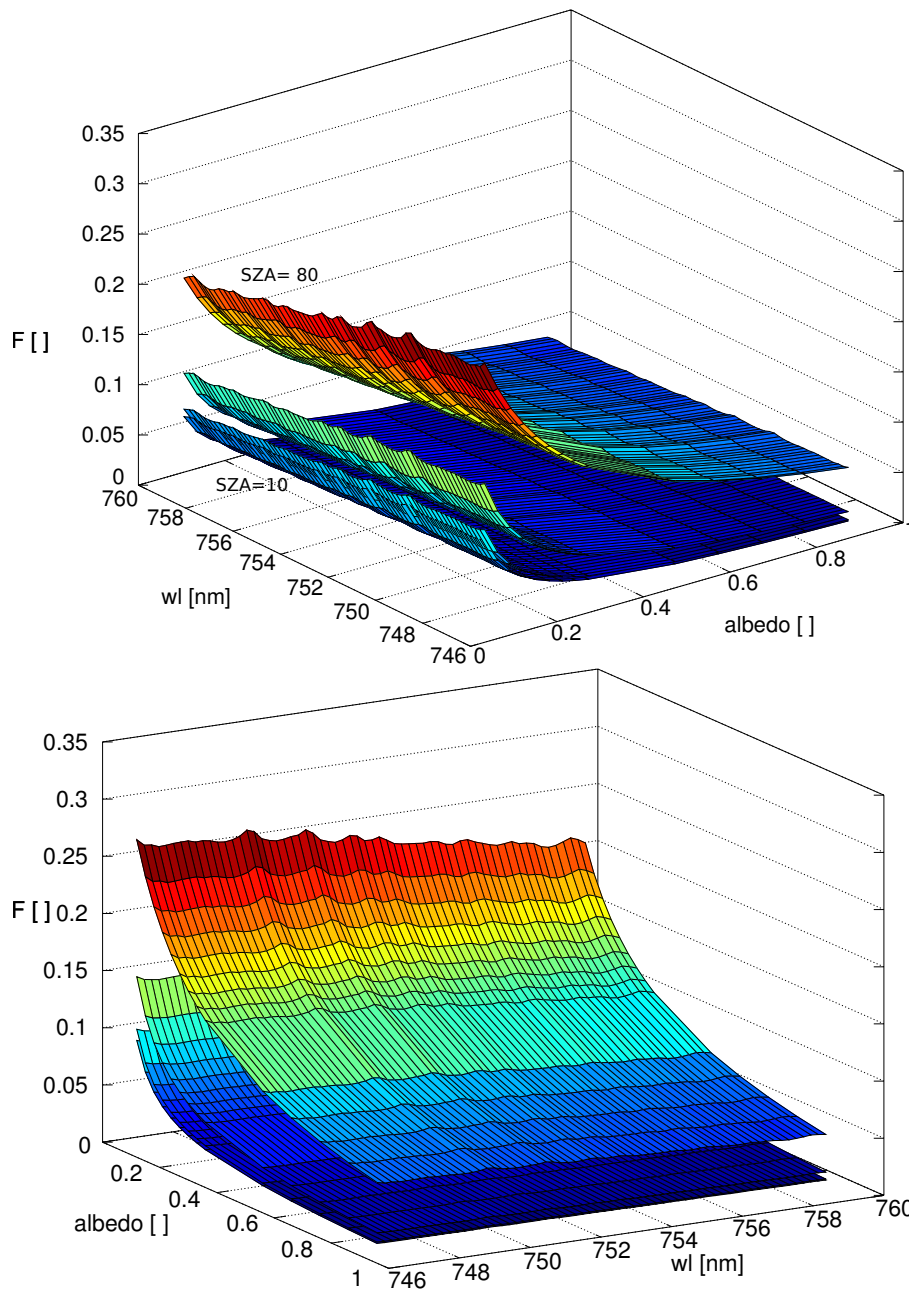


Figure 4.3: The change of fluorescence reference spectrum with respect to the ground reflection and solar zenith angles of 10,30,60 and 80 degrees. Both figures are showing the same plot from different perspectives and the surfaces with the same colors have the same F value. The color varies between red, for higher F values, to blue, for the low F values. The higher surface is for the solar zenith angle of 80 degrees and the lowest surface represents the solar zenith angle of 10 degrees which means sun is higher in the sky.

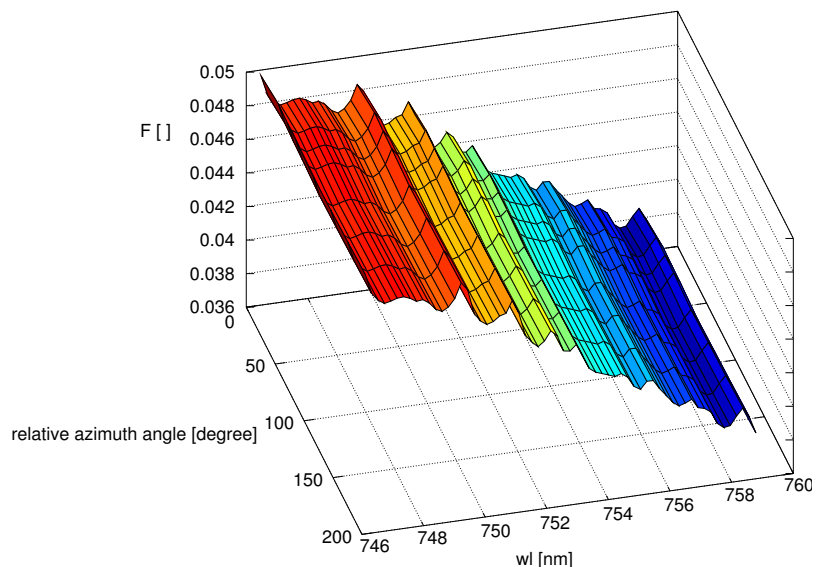


Figure 4.4: The variation of fluorescence reference spectrum, F , for the viewing angle of 30.0 degrees which is the larger viewing angle of SCIAMACHY in nadir mode with respect to relative azimuth angle variation. The same colors represent the same F values the same way they do in Fig. 4.1.

one, it means that the fluorescence reference spectrum, F , is properly adequate to the radiance I^+ and there is no need to suppress or stretch the reference spectrum, F .

A simple way to ensure that the most important terms are considered, is to check whether by inserting the most adequate absorber optical depth, light radiance intensity, I^+ , and fluorescence reference spectrum, F , the obtained fit factor, f , is equal to one.

To examine this idea, the retrieval concept was checked for the proper intensity, water vapor optical thickness, and fluorescence reference spectrum (all prepared for the same geophysical condition). So, f is obtained to be ~ 1.001 for the standard condition when all terms are adequate. So f , differs from one only by 0.1% which is a very good accuracy level for model runs. A candidate source of this small shift from 1.000 is the RRS.

4.1.6 Step 6: Sensitivity study considering RRS and the error study

According to the previous steps, the most important sources of inadequacy in fluorescence retrieval are the geophysical factors which dominate the background light I^- e.g. ground reflection or albedo. Therefore, it is necessary to understand how much can any error in the reflectance ($\sim I^-$) estimation, due to wrong ground reflection selection, affect the obtained fit factor f .

To test the influence of albedo error on the retrieved f , one way is to produce variety of I^+ and I^- by SCIATRAN by altering the ground reflection systematically

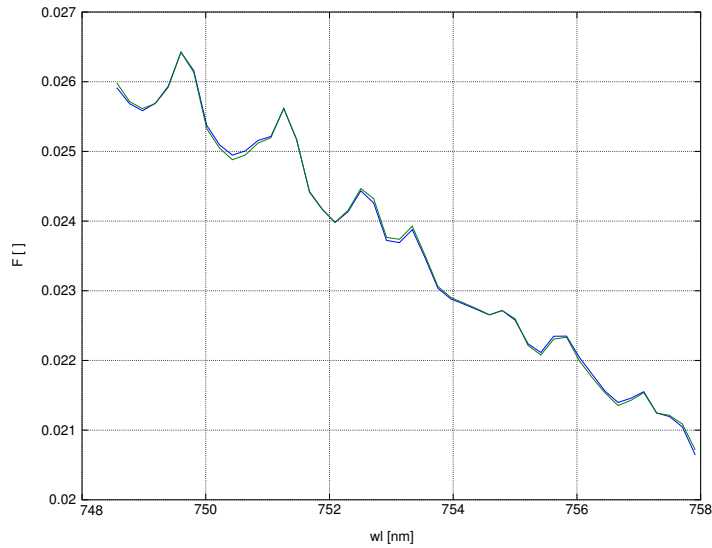


Figure 4.5: The fitted fluorescence optical depth, which is fitted by the retrieval approach, including the residual (*green line*), vs. fF , the product of f , as the retrieval output, and F represents the fluorescence OD (*blue line*).

and provide the fluorescence reference spectrum F for each couple of proper intensities having the same albedo. Inserting an adequate couple of I^+ and F (prepared based on similar albedo and using the same albedo as used in the F creation.) into the retrieval, is expected to have an output of $f = 1.001$. However, inadequacy between I^+ and F , which means having different albedo as initial condition, leads to $f \neq 1$.

This outcome, can be interpreted as a $X\%$ of error in the assumed ground reflection (albedo) leads to $Y\%$ of error in the retrieved fit factor f . Thus, the error study is done as follows:

In the case of real retrieval, albedo is a term which is not well-known before and can be a source of error. Two different ground reflection ratios are chosen to represent the high and low albedo for the green regions. The high albedo is chosen to be 0.3 (30% of the incident light is reflected back by the ground) and the low albedo is assumed to be 0.05 (5% of the incident light is reflected back by the ground). The albedo variation for both was 10% in each step *up to* 100% error for low albedo and *down to* -60% for high albedo.

According to Fig. 4.6 (blue lines) there is a linear dependency between the albedo and fluorescence fit factor errors and each 10% error in albedo estimation for low albedo reference = 0.05 leads to $\sim 5.5 - 6\%$ larger fluorescence fit factor, f , calculation. For high albedo reference = 0.30, when albedo is estimated 10% lower than 0.3, the fluorescence fit factor is $\sim 9 - 9.5\%$ smaller than the reference f .

The fluorescence offset impact correlates to the RRS infilling, it is important for fluorescence retrieval to know how it contributes to the RRS infilling.

Including the RRS into the model study, by means of providing the radiances and fluorescence reference spectrum, the obtained fit factor $f = 1.000$. Thus, the source of the small f variation from 1.000 in section 4.1.5 is known at the model level and the perfect adequacy has been reached.

However, the impact of the RRS on the fluorescence retrieval and the error contribution between fluorescence fit factor and RRS should be analyzed thoroughly. For this purpose, the same error study is done when RRS was also included in the radiance generated by SCIATRAN. Fig. 4.6 (green lines) show a slightly shifted linear error dependency between ground reflectance and retrieved fluorescence fit factor f . Nevertheless, the shift is not significant. Table 4.1 compares both conditions of presence and absence of RRS for the albedo error contribution to the fluorescence retrieval scaling factor, for the low reference albedo of 0.05. Table 4.2 compares both conditions of presence and absence of RRS for the albedo error contribution to the fluorescence retrieval scaling factor, for the high reference albedo of 0.3. From tables 4.1 and 4.2, it can be seen that according to the model results, the effect of RRS does not dominate the fluorescence retrieval significantly. However, to insure that the RRS infilling effect is not comparable with fluorescence impact on the retrieved spectral radiance, the model study is expanded into a high resolution study on a specific sample Fraunhofer line in section 4.2. The reason for limiting the study to only a single Fraunhofer line is that RRS infilling and fluorescence offset, correlate.

4.1.7 Discriminating between vegetation fluorescence and other luminescence signals

The last main test has been done on the retrieval method was to check whether it can recognize fluorescence among any possible interfering luminescence from different sources e.g. minerals from the bare soil/sand.

According to Gaft et al. (2005) (and personal correspondence (2012)), mineral luminescence is also a slowly varying spectral feature which can be within the same wavelength window as fluorescence for some minerals e.g. some iron ions.

Krbetschek et al. (1997) stated that the quartz sand from desert regions contains minerals having thermal and optical stimulation luminescence in the same wavelength window as our interest for fluorescence detection which might influence our retrieval. Therefore, the retrieval method is tested for an instance luminescence emission instead of the fluorescence, \mathcal{F} .

SCIATRAN's fluorescence double peak spectrum from Rascher et al. (2009), has an average power of $2.53 \text{ mW m}^2 \text{ sr}^{-1} \text{ nm}^{-1}$. \mathcal{F} has been replaced by a luminescence

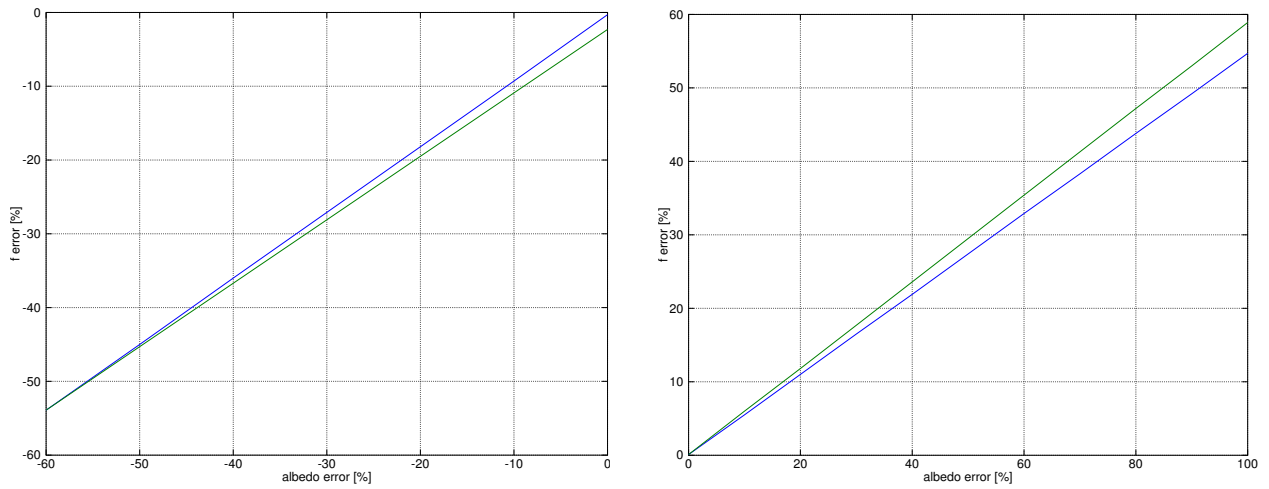


Figure 4.6: *Left*: The initial albedo is 0.30 and decreasing by 10% in each step. *Right*: The initial albedo is 0.05 and increasing by 10% in each step. The percentage of error on the fluorescence fit factor f due to inadequacy between the modeled received radiance I^+ and fluorescence reference spectrum, F , with respect to the error in estimating the ground reflection (albedo). The blue and the green lines show the f error when RRS is not taken into account (blue) and taken into account (green) for I^+ and F creation respectively. The difference between the two cases of presence and absence of RRS is not significant.

Table 4.1: The errors due to the albedo errors, for high albedo of 0.30, divided into two different cases of presence and absence of RRS effect.

albedo (%)	albedo error (%)	f error in absence of RRS (%)	f error in presence of RRS (%)
0.050	0	0.1	0.1
0.055	10	5.5	6.0
0.060	20	11.0	11.8
0.065	30	16.5	17.7
0.070	40	21.9	23.6
0.075	50	27.4	29.5
0.080	60	32.9	35.4
0.085	70	38.3	41.3
0.090	80	43.8	47.2
0.095	90	49.2	53.0
0.100	100	54.7	58.9

Table 4.2: The errors due to the albedo errors, for low albedo of 0.05, decided into two different cases of presence and absence of RRS effect.

albedo (%)	albedo error (%)	f error in absence of RRS (%)	f error in presence of RRS (%)
0.30	0	-0.3	-2.3
0.27	-10	-9.3	-10.9
0.24	-20	-18.2	-19.5
0.21	-30	-27.1	-28.1
0.18	-40	-36.0	-36.7
0.15	-50	-45.0	-45.3
0.12	-60	-53.9	-53.9

power spectrum, \mathcal{L} , being equal to 5% of the fluorescence average power, representing a weak mineral luminescence, which varies much slower than fluorescence within the spectral wavelength interval and can be assumed to be stationary. The output radiance I^+ from SCIATRAN is used in DOAS with the standard fluorescence reference spectrum, F , based on the fluorescence power. The received fluorescence scaling factor was $f \sim 0$. But, the RRS fit factor showed an increase of 50%; ($r = 1.49$) which means the weak luminescence is fitted as RRS effect. However for the standard fluorescence condition, adequate radiance, I^+ , produced based on \mathcal{F} , the fluorescence scaling factor was proposed to be 1.000 and the RRS scaling factor was negligible respectively.

Obtaining promising results from $\mathcal{L} = \text{constant} < \mathcal{F}$, the next step was to set \mathcal{L} with a higher value than the average fluorescence power, \mathcal{F} . It is chosen to be $3.00 \text{ mW m}^2 \text{ sr}^{-1} \text{ nm}^{-1}$ to be $\sim 20\%$ larger than \mathcal{F} . The fluorescence fit factor was negligible again ($f \sim 0$) and RRS scaling factor had a large value of ~ 11.61 which shows that the luminescence emission is fitted as RRS again.

The final test was to define a linearly variable luminescence spectral power representing a mineral luminescence slowly varying tail (Joiner et al., 2012), and compare the respective fit factors to the obtained fit factors from the constant \mathcal{L} . Thus, the luminescence \mathcal{L} decreasing linearly with respect to the wavelength, is defined as: $\mathcal{L}(\lambda) = -0.005 \lambda + 4.3 \text{ mW m}^2 \text{ sr}^{-1} \text{ nm}^{-1}$. The fluorescence fit factor is negligible again ($f \sim 0$) according to DOAS results and RRS fit factor has a relatively high

value (~ 2.93), which shows approximately three times scaling in RRS OD while fluorescence is not retrieved.

Hence, according to the model fluorescence retrieval, the mineral luminescence does not perturb the fluorescence retrieval significantly. Theoretically, luminescence should be fitted as RRS and not fluorescence because it correlates to RRS stronger than fluorescence.

To conclude the comparison between unknown luminescence, \mathcal{L} , and fluorescence, \mathcal{F} , can ensure that the model study shows a very promising feasibility for terrestrial vegetation fluorescence retrieving by DOAS with the SCIAMACHY spectral resolution.

4.2 Selected spectral window Model study

So far, the solar irradiance being used in the radiative transfer model, was the solar irradiance as SCIAMACHY measures. When monochromatic radiation * is received by the SCIAMACHY detector, it passes the slit and smoothed by the slit function to the instrument's spectral resolution for the selected channel. So, the features within smaller intervals than 0.48 nm are missing. Hence, the model results should be tested by a radiance created based on a high resolution solar irradiance to ensure the model results so far, are reliable.

As it has been mentioned earlier, RRS has an infilling effect on spectral absorption lines. Fluorescence also has an effect which cannot be defined as infilling, but an offset which fills the lines due to its slope as well. A Fraunhofer line can be selected within the fluorescence reference spectrum spectral window. F is defined by Eq. 2.6 and can be calculated for the selected Fraunhofer line which is extremely narrow and can approximately be written as:

$$(4.2) \quad \lim_{\delta\lambda \rightarrow 0} F = \lim_{\delta\lambda \rightarrow 0} \ln \frac{I^+(\delta\lambda)}{I^-(\delta\lambda)} = \frac{I^+(\delta\lambda) - I^-(\delta\lambda)}{I^-(\delta\lambda)}$$

$\delta\lambda$ represents a narrow wavelength window element.

To ensure that the monochromatic radiation features, which cannot be observed in the SCIATRAN model study based on SCIAMACHY solar irradiance measurements, cannot affect the SCIAMACHY data retrieval, the high resolution study is done based on another solar irradiance spectra from *Kurucz* irradiance measurement ([Kurucz et al., 1984](#)). The line-shape of the SCIAMACHY slit function is assumed to be a Gaussian function. Consequently, the smoothing function is chosen to be Gaussian, and the obtained smoothed radiance is compared to the radiance produced by SCIATRAN in the

*Electromagnetic radiation having wavelengths confined to an extremely narrow range.

same wavelength window, based on relatively low resolution solar irradiance measured by SCIAMACHY. Subsequently, the Fraunhofer line between 748.8 and 750.4 *nm* is selected as the *selected narrow window* to be tested. First, a reference setup is set for SCIATRAN with the following conditions:

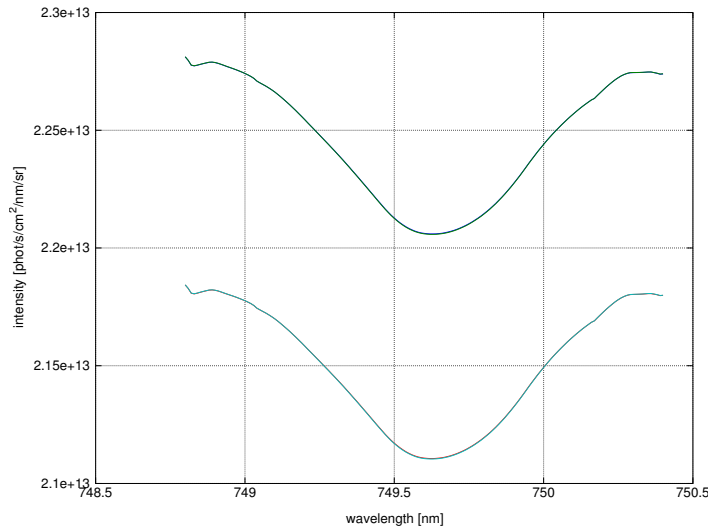
- ground reflectance or albedo = 0.15
- solar zenith angle= 30.0
- viewing angle= 0.1
- relative azimuth angle = 0.0
- aerosol OD = 0.59 for 749.0 *nm*.

Then, the radiance was produced for four different pre-defined conditions by changing the following terms within the standard condition; Presence/absence of fluorescence spectra and presence/absence of Ring effect. The results are plotted in Fig. 4.7 (a). According to the plots RRS and fluorescence have different effects on a certain Fraunhofer line. Fluorescence adds an offset to the line asymmetrically due to its slope and RRS fills the line center only as it rearranges the distribution of photons. Obviously, the in-filled intensity due to the RRS cannot compete to fluorescence additive features. This outcome is also followed by Fig. 4.7 (b) which shows the RRS infilling vs. fluorescence impact. Although fluorescence also fills the selected Fraunhofer line, the scale of fluorescence offset is almost two orders of magnitude larger than the RRS infilling effect. Obviously, RRS cannot be fitted as fluorescence according to the model.

4.2.1 The effect of albedo

To analyze the ground reflectance, albedo, on the fluorescence retrieval and its contribution to the RRS infilling, the whole experiment was repeated for a low albedo which is selected to be 0.08 and high albedo of 0.30. The chosen low/high albedo quantities are approximately two times larger and smaller than the reference albedo. The reference albedo represents the average albedo of the green areas within the fluorescence retrieval spectral window. The low albedo is considered to be for dark coniferous forests and the large albedo represents dry landscapes e.g. desert (Koelemeijer et al., 2003). The results are shown in Fig. 4.8. The upper plots are showing the large albedo effect on the selected Fraunhofer line and the bottom plots are showing the same for low albedo value. The right hand side plots show how the net effect of fluorescence differs from the RRS infilling. They also demonstrate that the fluorescence offset dominates the RRS infilling effect. As it can be seen from the figure, high albedo, leads to higher, and low albedo to lower retrieved radiance, respectively. In contrast,

a)



b)

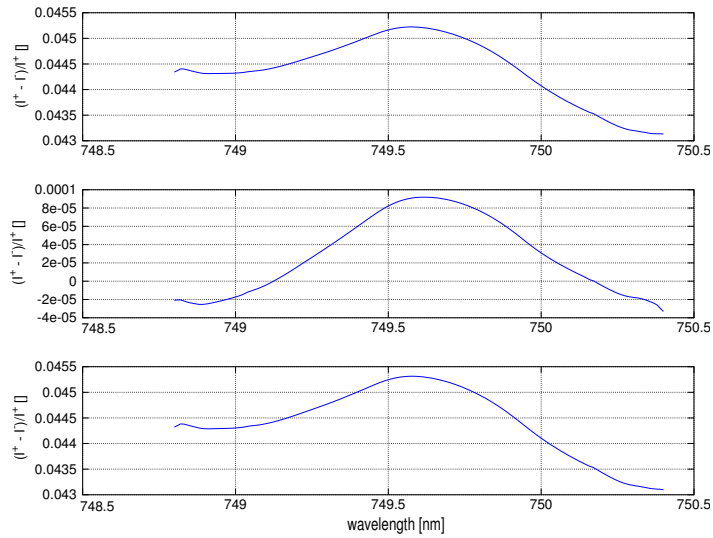


Figure 4.7: (a) shows the offset fluorescence applies on a single Fraunhofer line. The green Fraunhofer line is the blue one with the additive offset. The RRS infilling effect is negligible and hardly can be seen. looking at (b), the first plot represents the net effect of fluorescence is shown as $\frac{I^+ - I^-}{I^-}$ and is asymmetric, having a slope due to its variation. However, the RRS infilling can be seen from the second part, which is symmetric, distributed around zero and is more than 2 order of magnitude smaller than the fluorescence offset effect. The third part confirms it by adding up the RRS and fluorescence effect, which is practically the same as the first plot, being only fluorescence impact.

the high albedo lowers the fluorescence offset impact and vice versa. This means the increase of the albedo has a positive correlation to the intensity of retrieved light, but a decrease the wights of Ring and fluorescence retrievals. The outcome is predictable according to the sensitivity study (section 4.1.3), since the weight of a constant amount of additive photons is less on a higher radiance intensity. Thus, the sensitivity results are confirmed by the outcome of the high resolution albedo test.

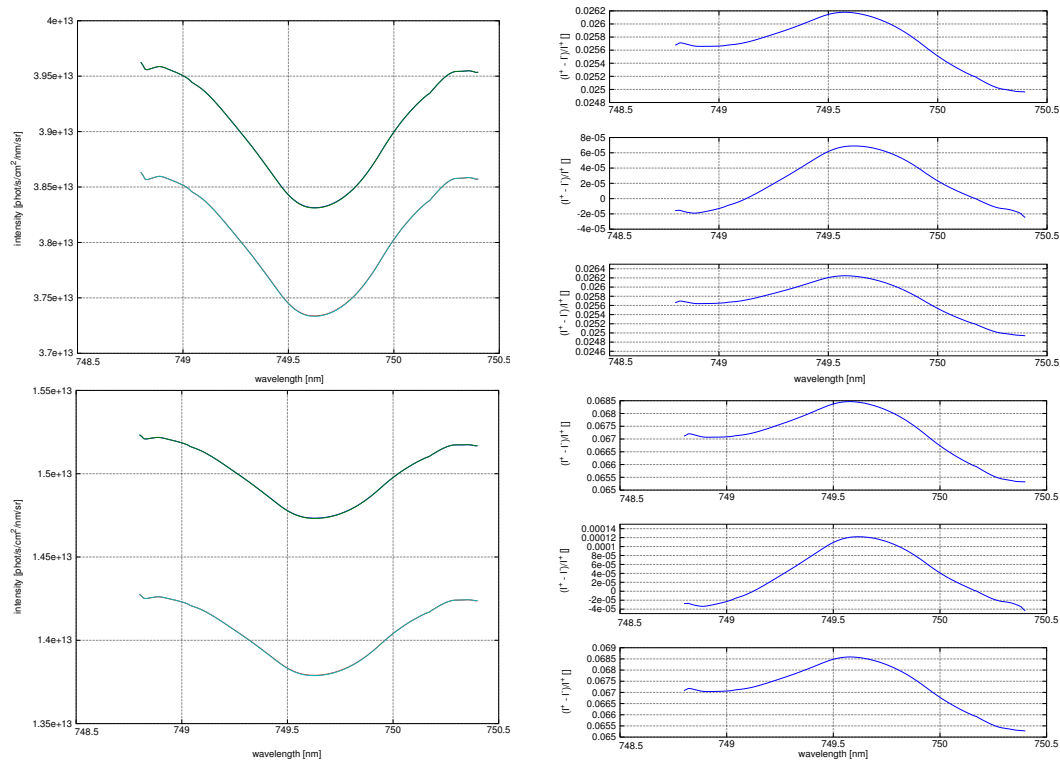


Figure 4.8: The upper plots represent the high albedo case and lower plots represent the low albedo case. upper-left → The offset fluorescence applies on a single Fraunhofer line for the *high albedo* case (green line vs. blue line). The RRS infilling effect is negligible and hardly can be seen. upper-right → For *high albedo* consists of three plots: The first plot represents the net effect of fluorescence is shown as $\frac{I^+ - I^-}{I^-}$ and has a slope due to its variation. However, the RRS infilling can be seen from the second part, which is symmetric, distributed around zero and is more than 2 orders of magnitude smaller than the fluorescence offset effect. The third part confirms it by adding up the RRS and fluorescence effect, which is practically the same as the first plot. However, as it can be seen, increasing the albedo by ~ 2 times leads to decreasing the fluorescence impact by a comparative scale. lower-left and lower-right → the same features for the *low albedo* case; the fluorescence offset effect from the right plot is two times smaller than the reference Fig. 4.7

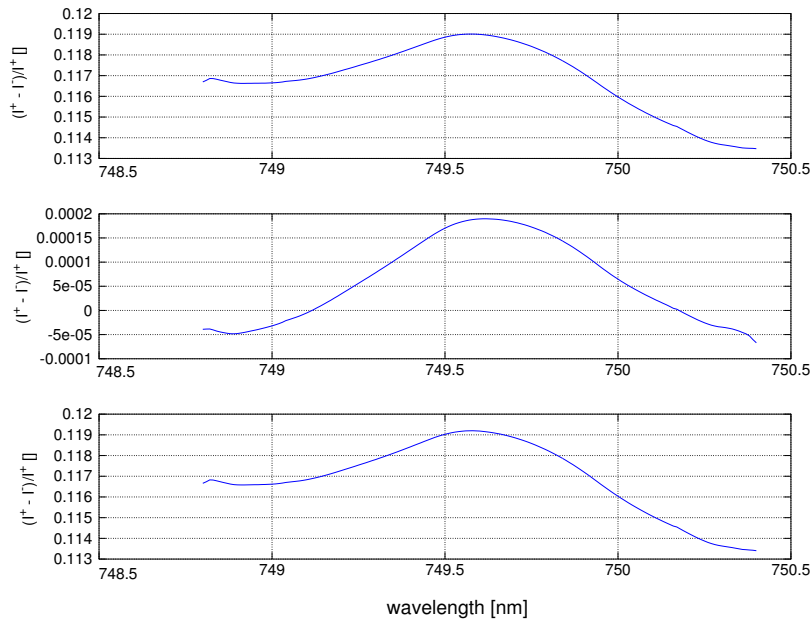


Figure 4.9: The solar zenith angle dependent fluorescence offset and RRS infilling. The upper plot represents the fluorescence net offset effect. The center plot shows the RRS infilling effect and from the lower plot the net impact of fluorescence and RRS can be seen.

4.2.2 The effect of solar zenith angle

From the sensitivity study it is known that solar zenith angle is also affecting the background radiance, I^- . Therefore, the same experiment for the selected single Fraunhofer line is repeated for large solar zenith angle of 75.0 degrees. The results are shown in Fig. 4.9, confirming the sensitivity results for the entire wavelength window. The larger the solar zenith angle becomes, the less the brightness is. Thus, large solar zenith angles increase the sensitivity of fluorescence and RRS retrieval. However, their impacts orders of magnitude are not comparable according to the model.

According to Fig. 4.9, the effect of large solar zenith angle is significant and the fluorescence impact is up to three times more than the reference fluorescence offset Fig. 4.7 and therefore, the RRS effect is larger than the reference RRS infilling but not comparative to fluorescence.

4.2.3 The effect of aerosols

The aerosol concentration, shielding the ground and increasing light scattering, is highly variable over vegetation, sand, ice etc. Therefore, the model experiment was repeated for two different aerosol optical thicknesses. Both aerosol optical depths (OD) were set at 749 nm for the selected Fraunhofer line as following:

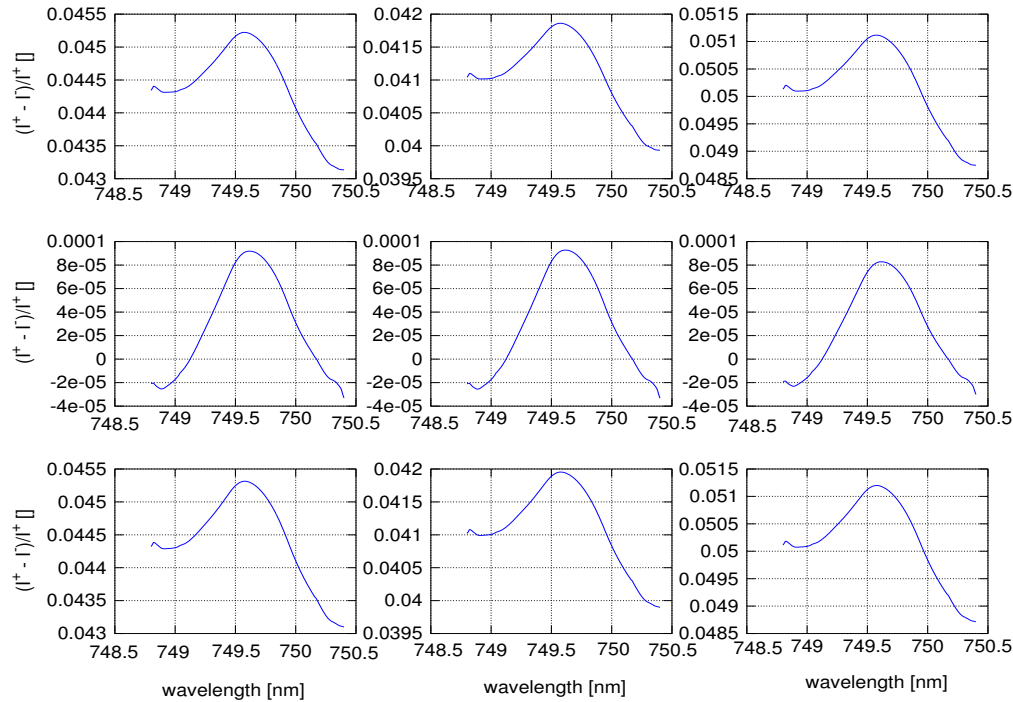


Figure 4.10: upper-left→ The reference fluorescence offset impact. upper-center→ The fluorescence offset impact for high aerosol OD. It shows slightly weaker net offset with respect to the reference. upper-right→ The fluorescence offset impact for low aerosol OD. It shows slightly stronger net offset with respect to the reference. The second row: right→ shows the reference RRS infilling. center→ shows the RRS infilling for high aerosol OD and left→ represents the RRS infilling for the low aerosol OD. There is no significant variation from left (reference) to the center (high aerosol OD) and to the right (low aerosol OD). The third row; represents the net effect of RRS and fluorescence left→ reference, center→ high aerosol OD and right →low aerosol OD.

- high aerosol OD= 0.83
- low aerosol OD= 0.01

According to the plotted results in Fig. 4.10, high aerosol OD leads to slightly higher and low aerosol OD to lower retrieved intensity respectively, for the same reason as in the case of the exchange of albedo and solar zenith angle. The expected negative correlation between the aerosol OD and the RRS/fluorescence spectral impact is confirmed as well. Fig. 4.10 also shows that practically the RRS infilling is negligible relative to fluorescence offset.

4.2.4 Special case; simulation 1: Sahara

As we expected no significant amount of vegetation in desert and ice covered areas, they are chosen as two extreme cases to be modeled on the narrow selected wavelength interval. The high reflectivity of these regions is due to different combinations of these major reflection causes; albedo, solar zenith angle and aerosol OD.

One specific optical property of Sahara or other desert-like regions is high red and NIR ground reflection, and often, there is a high aerosol concentration over deserts. Located in low latitudes and subtropics, the solar zenith angle is changing during the day but it can be small around noon. Typical desert condition has been modeled as follows:

- albedo= 0.30
- solar zenith angle= 30.0
- Aerosol OD= 0.83 for 749.0 nm

As it can be seen from plotted results in Fig. 4.11, the second column represents the desert like regions. The upper plot shows the fluorescence net offset to the selected Fraunhofer line. The center plot represents the RRS infilling again and the lower one shows their total infilling-behavior impact. The interference of high aerosol OD and large albedo increases the brightness, I^- , and decrease the weight of Ring infilling and fluorescence offset significantly.

4.2.5 Special case; simulation 2: Polar regions

For polar regions, located at high latitudes, solar zenith angle is usually large. Snow coverage causes high ground reflectivity, albedo. The aerosol concentration over polar regions is also lower than deserts. The modeled polar condition is as follows:

- albedo= 0.30
- solar zenith angle= 75.0
- Aerosol OD= 0.01 for 749.0 nm.

The right column of Fig. 4.11 represents the infilling-behavior of both RRS and fluorescence. The upper plot is again the fluorescence offset effect, the center one is the RRS infilling and the lower one is the summation of both impacts. Obviously, the fluorescence offset has stronger impact than RRS as before. The between desert-like areas and polar regions can be seen by comparing Fig. 4.11 right column for the polar condition and Fig. 4.11 center column for desert-like condition. Low aerosol OD is not increasing the brightness, I^- , but large albedo is. In addition, the interference

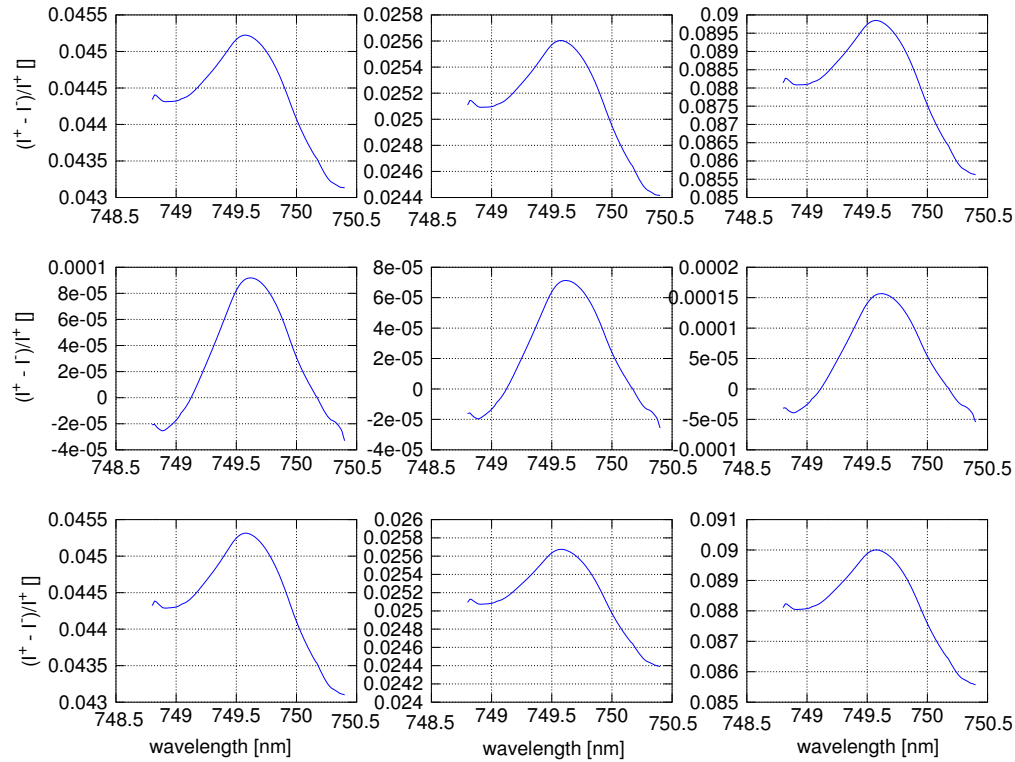


Figure 4.11: upper-left→ The reference fluorescence offset impact. upper-center→ The fluorescence offset impact for sub-tropical deserts. It shows significantly weaker net offset with respect to the reference. upper-right→ The fluorescence offset impact for polar regions. It shows significantly stronger net offset with respect to the reference. The second row shows the RRS infilling for right→ reference condition, center→ desert and left→ polar regions. The third row represents the net effect of RRS and fluorescence left (reference), center (Desert) and right (polar regions).

between large albedo and large solar zenith angle is destructive as well. Therefore, the surface brightness impact on F , is not as strong as desert condition. The large solar zenith angle is the dominating factor in polar regions according to Fig. 4.11 and leads to an overall enhancement of Ring infilling and fluorescence impact. Looking at the second row of Fig. 4.11, there is also significant variation for RRS infilling due to the albedo and solar zenith angle brightness for reference, desert and polar regions. From the third row, one can see that practically RRS infilling is negligible relative to fluorescence offset as we expected.

The obtained results from selected interval modeling of the two extreme cases of the desert-like and polar regions, show that large solar zenith angle and low aerosol OD can thwart the high albedo effect and lead to a significant fluorescence reference spectrum, F . In contrast, desert, having large albedo, small solar zenith angles dur-

ing the day, and high aerosol OD, appear significantly bright and consequently, the calculated F is relatively weak.

The high resolution model results, does not indicate any significant difference from the previous results. Therefore the modeled results, based on solar irradiance, measured by SCIAMACHY with spectral resolution of 0.48, are seem to be reliable.

Chapter 5

SCIAMACHY data study

Based on the promising results from the model study, the application to the real radiance measurement by SCIAMACHY (see section 3.3) is the next step.

Choosing the same spectral wavelength window for SCIAMACHY data, the measured radiance should be used in the retrieval method for fluorescence retrieval instead of the modeled I^+ prepared by SCIATRAN. However, the utilized fluorescence reference spectrum remains the modeled F which should be scaled based on fitting fluorescence from real radiances (see section 1.4).

For this purpose, the retrieval approach has been applied to the globally measured radiances from SCIAMACHY. The important absorber in this wavelength interval is water vapor which has a few shallow absorption lines within the wavelength interval. Therefore, a water vapor spectrum is fitted as well. A fixed RRS reference spectrum, as is standard in DOAS, a polynomial for eliminating the scattering features, and a fluorescence reference spectrum is set into the retrieval method. However, there are two different levels of complexity for the utilized fluorescence reference spectrum;

When F is non-variable :

As the first step, the fluorescence reference spectra has been fixed for all the ground pixels, independent on the geophysical and environmental conditions during the measurement. A strict cloud filter, based on a brightness threshold is also applied to eliminate the scattering and high reflectivity of clouds.

Thus, an average condition has been defined as the reference and a unique fluorescence reference spectrum F is provided for this standard condition. The properties of this reference condition is:

- ground reflection *albedo* = 0.30
- aerosol OD for 749.0 nm spectral wavelength= 0.01
- solar zenith angle = 30.0

- relative azimuth angle = 0.0
- viewing angle = 0.1

Fig. 5.1 versus Fig. 5.2 show poor fluorescence OD fit over the ground pixel which is marked by a red star and a good fit over a ground pixel which is specified with a green star at Fig. 5.3. The gray lines are the retrieved OD including the residual and the black lines represent the fitted OD by means of the fF product.

The reason for the poor fit is not clearly known but can be some unexpected thin clouds, which are not eliminated by the cloud filter. Another possible reason can be the flood-lands and the water interference.

The obtained global fit factors, f , having a fixed fluorescence reference spectrum, are shown Fig. 5.4 and Fig. 5.5. A clear seasonal change can be seen from the mapped fit factors f , looking at summer and winter maps. vegetated areas are shown bright and non-vegetated regions are dark. The minus sign is because an *emission cross section* used in DOAS as an *absorption cross section*. Therefore a negative f means it is not absorption but emission. When f is smaller than one, $f < 1$, F should be suppressed and when f is larger than one, $f > 1$, F should be stretched. However, the results are relative to the applied fluorescence reference spectrum. The only interpretation of the relative mapped f values is that, such fixed fluorescence reference spectrum should be scaled by these values to represent the retrieved fluorescence OD from the measured radiance spectrum for each ground pixel.

When F is variable Nevertheless, according to the model results, the measurement geophysical parameters dominate the fluorescence reference spectrum. For each ground pixel of measured radiance, the most appropriate F is utilized as the fluorescence reference spectrum. The proper F for an individual ground pixel is chosen by setting the most adequate F with respect to the aerosol OD, albedo, measurement geometrical properties, the sun geometry, season and latitude.

Yet, the interpretation of the obtained fluorescence scaling factors f is difficult due to the variation of the reference spectrum. Indeed, the scaling factor is highly dependent on the scaled reference spectrum and can vary widely.

A reason for such an outcome can be the influence of the background radiance, interfering with the retrieval. As it has been shown in the sensitivity study, the larger the background radiance is, the smaller are the values for fluorescence reference spectrum.

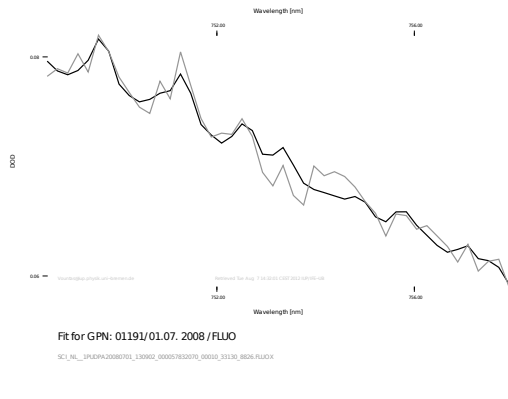


Figure 5.1: A good fluorescence OD fit to the retrieved fluorescence for the ground pixel shown by green star in Fig. 5.3. This ground pixel is in a green area, in south America. the latitude and longitude can be found on the map.

Figure 5.2: A poor fluorescence OD fit to the retrieved fluorescence for the ground pixel shown by red star in Fig. 5.3. The latitude and longitude can be found on the map.

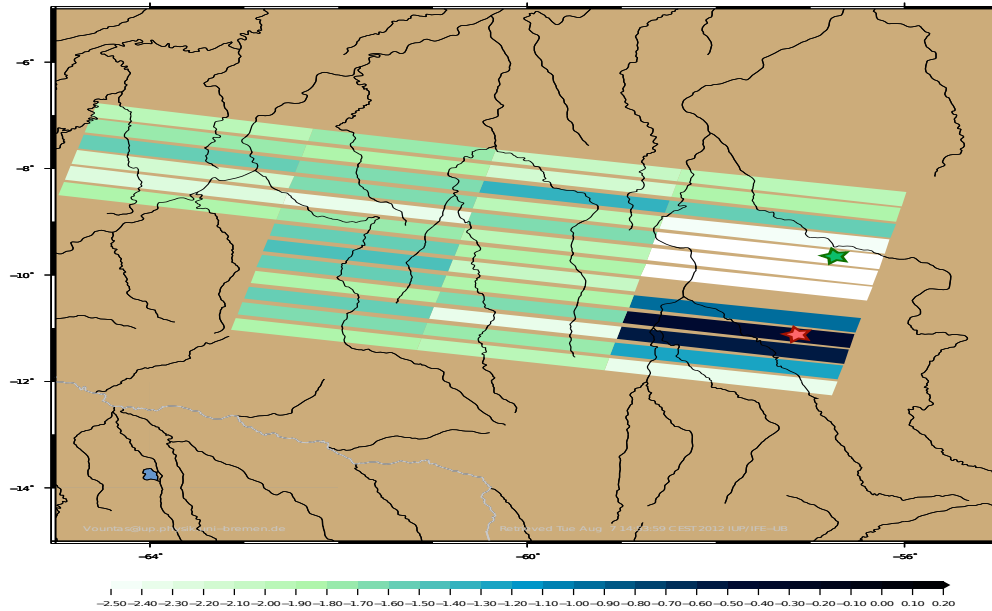


Figure 5.3: A sample of ground pixels, measured by SCIAMACHY over south America. The selected ground pixels as good and poor fluorescence OD fit are marked by a green and a red star respectively.

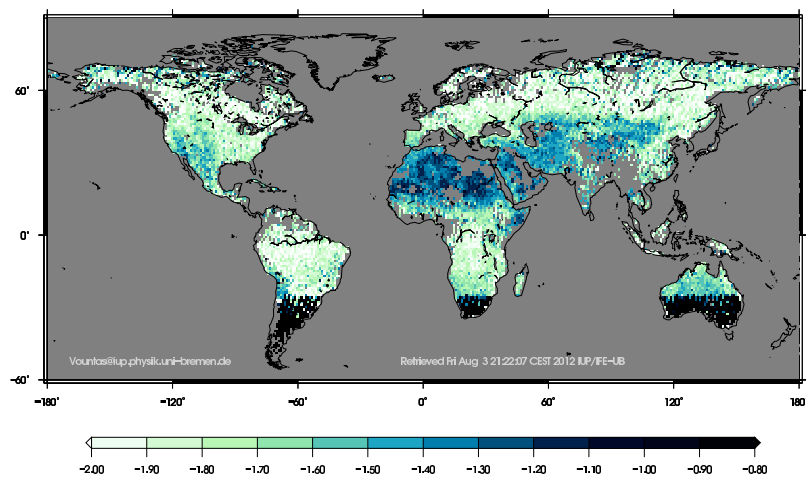


Figure 5.4: The global fluorescence fit factors f from real SCIAMACHY radiances, for a standard fluorescence reference spectrum F for the summer time from 01.06.2008 to 31.08.2008, averaged and gridded to obtain a softened map. In average each pixel is the average of 3-9 SCIAMACHY ground pixels.

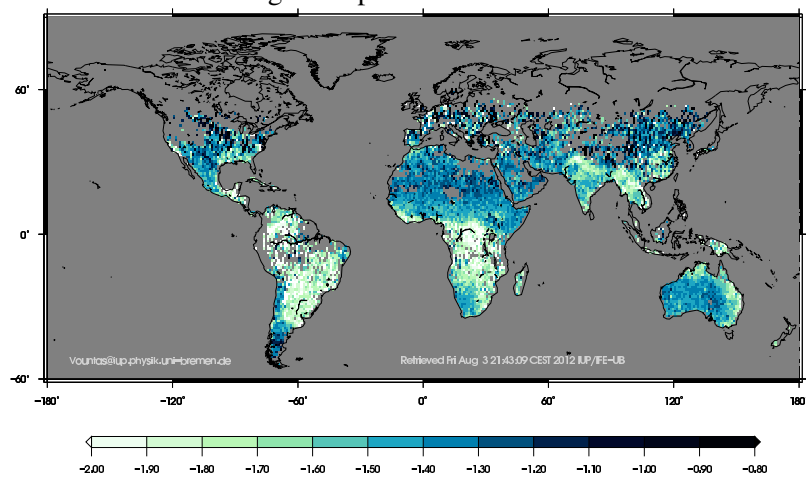


Figure 5.5: The global fluorescence fit factors f from real SCIAMACHY radiances, for a standard fluorescence reference spectrum F for the winter time from 01.01.2008 to 30.03.2008, averaged and gridded to obtain a softened map. In average each pixel is the average of 3-9 SCIAMACHY ground pixels.

Chapter 6

Summary conclusion and outlook

The terrestrial vegetation fluorescence has been measured in-situ and air-borne before ([Meroni et al., 2009](#)). Recently, plant fluorescence was being retrieved from space-borne measurements as well. Some new retrieval methods are developed to enable us to retrieve fluorescence faster and easier from satellite data ([Frankenberg et al., 2011](#); [Mazzoni et al., 2010](#); [Joiner et al., 2012, 2011](#); [Guanter et al., 2007, 2010](#)). Within this master thesis, the plant fluorescence is retrieved based on a relatively simple and fast method, DOAS (Differential Optical Absorption Spectroscopy), which is originally used for trace gas retrieval.

The study has been divided into two main parts:

- By simulating the impact of fluorescence on TOA upwelling radiances, we retrieved vegetation fluorescence at the modeling level.
- We applied of the modeling results on the real radiance measured by SCIAMACHY and retrieved the fluorescence.

The main focus of the model study was to simulate the spectral features, detected by the satellite instrument, using a radiative transfer model. The second step was to show the feasibility of DOAS, to discriminate between fluorescence and other spectral features.

The chosen radiative transfer model for the model study was SCIATRAN V3.1 including a fluorescence module prepared by [Rozanov \(2011\)](#).

As plant fluorescence provides a weak radiance relative to deep atmospheric absorption lines, a short wavelength interval near O₂-A absorption band is selected which has the least absorption features within the spectral window of interest. The absorption features are from water vapor and are difficult to detect with SCIAMACHY spectral resolution.

Within the model study the influence of plant fluorescence on the radiances at TOA is investigated. According to the modeling results, fluorescence adds an offset to the spectral features, due to its slope, as well as a pseudo filling in the Fraunhofer lines.

To be able to adapt DOAS to the fluorescence retrieval a fluorescence reference spectrum, F , was defined and created by rationing the simulated radiances including and excluding fluorescence (I^+ and I^- , respectively) and taking the logarithm of the product. This reference spectrum is fitted as a fluorescence emission cross section in retrieval. It is scaled by a factor of f , due to the retrieved fluorescence spectral features. The net effect of fluorescence emission on the received radiance at TOA was found to be an offset, shifting the radiance by adding some features, due to its slow-variation with respect to wavelength.

Using DOAS to retrieve fluorescence from modeled radiances, showed feasibility to retrieve fluorescence among all the absorption, elastic and in-elastic scattering features. It is also possible to distinguish between fluorescence and typical luminescence radiances, coming from different sources e.g. minerals by fitting them as Rotational Raman Scattering.

In addition, a sensitivity study was implemented to investigate all the geophysical and environmental parameters, which can influence the retrieval. The main outcome of the sensitivity study was that the more intense is the received radiance, the more difficult it is to retrieve fluorescence features. Particularly, another outcome is that the brighter the surface is, the smaller is the weight of a specific fluorescence offset value. Besides, using a fixed fluorescence reference spectrum F , the *relative* fluorescence scaling factor f was mapped globally and showed reasonable values in retrieving fluorescence. The high and low f values correctly represent the vegetated and non-vegetated regions.

However, the application of the method, using a *variable* F with respect to the geophysical and environmental conditions on the SCIAMACHY data, showed some confusions due to the interfering of the surface brightness variation for different ground pixels.

There are further steps to proceed which have not been performed due to the temporal limitation of this project;

- As it has been mentioned before, the obtained fluorescence fit factors, f , when the utilized F is not constant, are difficult to interpret because the scaled reference spectrum is not the same for every ground pixel. A possible solution could be to try Weighting Function modified DOAS (WF-DOAS) which has been developed by [Buchwitz et al. \(2000\)](#). Since, WF-DOAS uses a modeled vs. measured radiance instead of I_0 vs. measured radiance the effects of background light intensity could potentially be minimized.

- One of the probable reasons for receiving some deviated values of f for desert-like regions is the mineral luminescence (Joiner et al., 2012). Although DOAS has been checked for this issue and showed promising results at the model study level, a recommendation is to use NDVI (Normalized Difference Vegetation Index) and define different fluorescence spectrum for different bioms and assume no vegetation fluorescence over desert regions.
- An assessment of the results should be tested by doing a long term data validation study, using SCIAMACHY, Global Ozone Monitoring Experiment (GOME) and GOME-2 data.
- An important new concept can be a parallel Bio-chemistry study on photosynthesis reaction and obtain the reaction rate of the *light reaction*, in which fluorescence is emitted. Therefore, the rate of fluorescence can be determined and be compared to the light absorption rate. The goal is to find the the overall rate of photosynthesis. This can be a good indicator for CO₂ up-taking by plants. In addition, it can be possible to find the contribution between land and ocean CO₂ uptake. The utilization of such a modeling can be utilized in climate models (Burrows, 2012, personal correspondence).

Appendix A

Geophysical space-borne measurement geometrical properties

In SCIATRAN, the measurement geometry at Top Of Atmosphere (TOA) is defined by selecting these main terms as shown in Fig. [A.1](#):

When observing a point on the Earth from a satellite-based instrument at TOA, the Solar Zenith Angle, θ_0 , is the angle between the local zenith, i.e. directly above the point on the ground, and the line of sight from the observed point on Earth to the sun.

In the same way, the angle between the local zenith, which is nadir from satellite point of view, and the line of sight from the satellite to the observed point on Earth, is called the viewing (zenith) angle, θ .

Solar plain is defined as the plane which includes three specific point of the earth center, observation point and the sun.

An azimuth angle is generally calculated on the ground and from the north direction. The solar azimuth angle is the angle between north and the sun image on Earth. The satellite azimuth angle is also defined in the same way which means it is the angle between the north direction and the satellite image on Earth. The relative azimuth angle, ϕ , is defined as the angle between the solar plain and the satellite image on the ground.

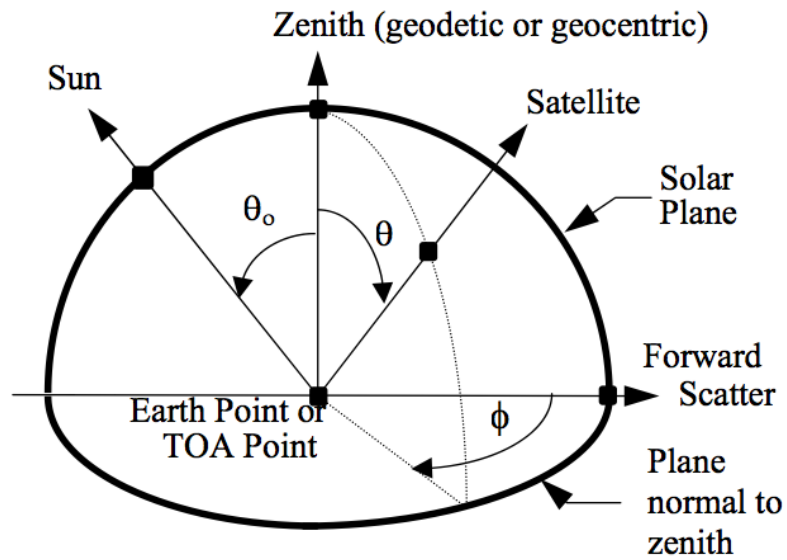


Figure A.1: The space-borne measurement geometry: ϕ = relative azimuth angle, θ = viewing (zenith) angle, θ_0 = solar zenith angle

Bibliography

- Bassham, J. and Calvin, M. (1957). *The path of carbon in photosynthesis*. Prentice-Hall.
- Bovensmann, H., Burrows, J. P., Buchwitz, M., Frerick, J., Nothmann, S., Rozanov, V. V., Chance, K. V., and Goede, A. H. P. (1999). SCIAMACHY - mission objectives and measurement modes. *J. Atmos. Sci.*, 56.
- Bracher, A. (Winter term 2011-2012). Ocean optics and ocean color remote sensing. http://www.iup.physik.uni-bremen.de/~bracher/ocean_color.
- Buchwitz, M., Rozanov, V. V., and Burrows, J. P. (2000). A near-infrared optimized doas method for the fast global retrieval of atmospheric ch₄, co, co₂, h₂o, and n₂o total column amounts from sciamachy envisat-1 nadir radiances. *Journal of Geophysical Research*, 105(D12).
- Elachi, C. and van Zyl, editors (2010). *Introduction to the Physics and Techniques of Remote Sensing*. John Wiley & Sons, 2nd edition.
- European Space Agency (2012a). Envisat homepage - [esa-https://earth.esa.int/web/guest/missions/esa-operational-eo-missions/envisat](https://earth.esa.int/web/guest/missions/esa-operational-eo-missions/envisat). Technical report, ESA.
- European Space Agency (2012b). Meris homepage - [esa-https://earth.esa.int/web/guest/missions/esa-operational-eo-missions/envisat/instruments/meris](https://earth.esa.int/web/guest/missions/esa-operational-eo-missions/envisat/instruments/meris). Technical report, ESA.
- Frankenberg, C., Butz, A., and Toon, G. C. (2011). Disentangling chlorophyll fluorescence from atmospheric scattering effects in o₂ a-band spectra of reflected sun-light. *Geophys. Res. Lett.*, 38.
- Gaft, M., Reisfeld, R., and Panczer, G. (2005). *Luminescence Spectroscopy Of Minerals And Materials*. Springer.
- Gottwald, M. and Bovensmann, H. (2011). *Sciamachy - Exploring the Changing Earth's Atmosphere*. Springer.

- Guanter, L., Alonso, L., Gomez-Chova, L., Amores, J., V., and Moreno, J. (2007). Estimation of solar-induced vegetation fluorescence from space measurements. *Geophys. Res. Lett.*
- Guanter, L., Alonso, L., Gomez-Chova, L., Meroni, M., Preusker, R., Fischer, J., and Moreno, J. (2010). Developments for vegetation fluorescence retrieval from spaceborne high-resolution spectrometry in the o2-a and o2-b absorption bands. *J. Geophys. Res.*, 115.
- Heldt, H. and Piechulla, B. (2010). *Plant Biochemistry*. Academic Press.
- Joiner, J., Yoshida, Y., Vasilkov, A. P., Middleton, E. M., Campbell, P. K. E., Yoshida, Y., Kuze, A., and Corp, L. A. (2012). Filling-in of far-red and near-infrared solar lines by terrestrial and atmospheric effects: simulations and space-based observations from sciamachy and gosat. *Atmospheric Measurement Techniques Discussions*, 5(1):163–210.
- Joiner, J., Yoshida, Y., Vasilkov, A. P., Yoshida, Y., Corp, L. A., and Middleton, E. M. (2011). First observations of global and seasonal terrestrial chlorophyll fluorescence from space. *Biogeosciences*, 8(3):637–651.
- Kaiser, G. E. (2001). Noncyclic photophosphorylation. <http://student.ccbcmd.edu/gkaiser/biotutorials/photosyn/fg4.html>.
- Koelemeijer, R. B. A., de Haan, J. F., and Stammes, P. (2003). A database of spectral surface reflectivity in the range 335-772 nm derived from 5.5 years of gome observations. *JOURNAL OF GEOPHYSICAL RESEARCH*, 108(D2).
- Krbetschek, M., Götze, J., Dietrich, A., and Trautmann, T. (1997). Spectral information from minerals relevant for luminescence dating. *Radiation Measurements*, 27(5-6):695 – 748.
- Kurucz, R., Furenhild, I., Brault, J., and Testermann, L. (1984). Solar flux atlas from 296 to 1300 nm, national solar observatory atlas no. 1, national solar observatory, sunspot, NM, USA.
- Mazzoni, M., Falorni, P., and Verhoef, W. (2010). High-resolution methods for fluorescence retrieval from space. *Opt. Express*, 18.
- Meroni, M., Rossini, M., Guanter, L., Alonso, L., Rascher, U., Colombo, R., and Moreno, J. (2009). Remote sensing of solar-induced chlorophyll fluorescence: Review of methods and applications. *Remote Sensing of Environment*, 113(10):2037 – 2051.

- NatureEducation webpage (2010). The light and dark reactions in the chloroplast. <http://www.nature.com/scitable/content/the-light-and-dark-reactions-in-the-14705803>.
- Platt, U. and Stutz, J. (2007). *Differential Optical Absorption Spectroscopy: Principles and Applications*. Physics of Earth And Space Environments. Springer.
- Rascher, U., Agati, G., Alonso, L., Cecchi, G., Champagne, S., Colombo, R., Damm, A., Daumard, F., de Miguel, E., Fernandez, G., Franch, B., Franke, J., Gerbig, C., Gioli, B., Gómez, J. A., Goulas, Y., Guanter, L., Gutiérrez-de-la Cámara, O., Hamdi, K., Hostert, P., Jiménez, M., Kosvancova, M., Lognoli, D., Meroni, M., Miglietta, F., Moersch, A., Moreno, J., Moya, I., Neininger, B., Okujeni, A., Ounis, A., Palombi, L., Raimondi, V., Schickling, A., Sobrino, J. A., Stellmes, M., Toci, G., Toscano, P., Udelhoven, T., van der Linden, S., and Zaldei, A. (2009). Cefles2: the remote sensing component to quantify photosynthetic efficiency from the leaf to the region by measuring sun-induced fluorescence in the oxygen absorption bands. *Biogeosciences*, 6(7):1181–1198.
- Rozanov, V. (2011). Sciatran (radiative transfer model and retrieval algorithm), version 3.1. Technical report, IUP, Bremen, Institute of Remote Sensing, University of Bremen, Germany.
- Sadeghi, A. (2012). *Phytoplankton Functional Groups from Hyperspectral Satellite Data and its Application for Studying Phytoplankton Dynamics in Selected Oceanic Regions*. PhD thesis, IUP, University of Bremen.
- Vountas, M. (1999). *Die Modellierung und Parametrisierung des Ring-Effektes: Einfluß auf die Bestimmung von stratosphärischen Spurengasen*. Berichte aus der Umweltwissenschaft. Shaker.
- Wheeler, R. (2010). leaf structure. <http://www.richardwheeler.net/contentpages/index.php>.

Index

B		T	
Beer-Lambert's law	12	Thylakoid	7
C		V	
Chlorophyll	7	Vibrational Raman Scattering (VRS) ..	15
chloroplast	7		
cross section	12		
D			
dark reaction	10		
F			
fluorescence reference spectrum	16		
Fraunhofer lines	15		
I			
Inelastic scattering	14		
Irradiance	12		
L			
light reaction	10		
M			
Mie scattering	14		
P			
photo-system	11		
R			
Radiance	11		
Radiative transfer equation	12		
Rayleigh scattering	14		
Rotational Raman Scattering (RRS) ..	15		
S			
singlet state	7		